University of Kent

Kent Academic Repository

Brazhnik, Evgeni A., Yildirim, Elena A., Gorfunkel, Elena P., Laptev, Georgi Yu., Tiurina, Darya G., Morozov, Vitali Yu., Filippova, Valentina A., Ilina, Larisa A., Sokolova, Kseniya A., Zaikin, Vasiliy A. and others (2026) ***Exploratory comparative ovarian transcriptomic profiling in Dekalb White hens identified candidate signatures associated with egg-laying plateau persistence.*** **Poultry, 5 (6). ISSN 2674-1164.**

Downloaded from

https://kar.kent.ac.uk/117577/ The University of Kent's Academic Repository KAR

The version of record is available from

https://doi.org/10.3390/poultry5060077

This document version

Publisher pdf

DOI for this version

Licence for this version

UNSPECIFIED

Additional information

Versions of research works

Versions of Record

If this version is the version of record, it is the same as the published version available on the publisher's web site. Cite as the published version.

Author Accepted Manuscripts

If this document is identified as the Author Accepted Manuscript it is the version after peer review but before type setting, copy editing or publisher branding. Cite as Surname, Initial. (Year) 'Title of article'. To be published in ***Title of Journal*** , Volume and issue numbers [peer-reviewed accepted version]. Available at: DOI or URL (Accessed: date).

Enquiries

If you have questions about this document contact ResearchSupport@kent.ac.uk. Please include the URL of the record in KAR. If you believe that your, or a third party's rights have been compromised through this document please see our Take Down policy (available from https://www.kent.ac.uk/guides/kar-the-kent-academic-repository#policies).

poultry

MDPI

Article

Exploratory Comparative Ovarian Transcriptomic Profiling in Dekalb White Hens Identified Candidate Signatures Associated with Egg-Laying Plateau Persistence

Evgeni A. Brazhnik [1], Elena A. Yildirim [2,3], Elena P. Gorfunkel [2], Georgi Yu. Laptev [2], Daria G. Tiurina [2], Vitali Yu. Morozov [3], Valentina A. Filippova [2,3], Larisa A. Ilina [2,3], Kseniya A. Sokolova [2,3], Vasiliy A. Zaikin [2], Alesya A. Savicheva [2], Valeria A. Kalmykova [2,3], Ksenia N. Timofeeva [2], Polina V. Grek [2], Alexandra Y. Burlakova [2], Olga A. Mironova [4,5], Darren K. Griffin [6,7,8] and Michael N. Romanov [7,8,9,*]

1 Federal State Budgetary Scientific Institution "Agrophysical Research Institute", St. Petersburg 195220, Russia; brazhnik@agrophys.ru
2 Molecular Genetics and Microbiomics Laboratory, BIOTROF+ Ltd., Pushkin, St. Petersburg 196602, Russia; deniz@biotrof.ru (E.A.Y.); alenkafev@mail.ru (E.P.G.); georg-laptev@rambler.ru (G.Y.L.); tiurina2@biotrof.ru (D.G.T.); filippova@biotrof.ru (V.A.F.); ilina@biotrof.ru (L.A.I.); kseniya.k.a@biotrof.ru (K.A.S.); dfcx@biotrof.ru (V.A.Z.); sava@biotrof.ru (A.A.S.); lera@biotrof.ru (V.A.K.); timofeevaks@biotrof.ru (K.N.T.); grekpv@biotrof.ru (P.V.G.); alexb@biotrof.ru (A.Y.B.)
3 Federal State Budgetary Educational Institution of Higher Education, St. Petersburg State Agrarian University, Pushkin, St. Petersburg 196605, Russia; supermoroz@mail.ru
4 Basic Department of Phytosanitary Biology and Ecosystem Safety, Institute of Ecology, Federal State Autonomous Educational Institution of Higher Education "Patrice Lumumba Peoples' Friendship University of Russia", Moscow 117198, Russia; mironova-olan@rudn.ru
5 Federal State Budgetary Institution "All-Russian Plant Quarantine Center" (Federal State Budgetary Institution "VNIIKR"), Urban-Type Settlement Bykovo, Ramenskoye 140150, Russia
6 Preimplantation Genetics Group, EGA Institute for Women's Health, University College London, London WC1E 6HX, UK; darren.griffin@ucl.ac.uk
7 School of Natural Sciences, University of Kent, Canterbury CT2 7NJ, UK
8 Animal Genomics and Bioresource Research Unit (AGB Research Unit), Faculty of Science, Kasetsart University, Chatuchak, Bangkok 10900, Thailand
9 L. K. Ernst Federal Research Center for Animal Husbandry, Dubrovitsy, Podolsk Urban Okrug 142132, Russia
* Correspondence: m.romanov@kent.ac.uk

Abstract

The peak egg-laying plateau in poultry is regulated by complex genetic factors. To elucidate these, we performed a comparative ovarian transcriptome profiling (RNA-Seq) of Dekalb White hens with distinct egg production curves, using early-persistent (PP, $n = 3$) vs. late-degraded (DP, $n = 3$) birds selected by contrasting phenotypes from 60 birds per cohort at 49.5 weeks of age. PP hens showed earlier plateau onset (24 vs. 27 weeks), higher production (97.32% vs. 85.43%), lower body weight (1652.27 ± 26.19 vs. 1869.05 ± 32.18 g) and lower liver weight (34.85 ± 2.55 vs. 44.55 ± 1.10 g) than DP birds ($p < 0.05$). Suggestive shifts in hematological profiles (erythrocytes, hemoglobin, color index) were observed in the DP group ($p < 0.05$). Among 17,285 loci, 484 differentially expressed genes were identified (305 upregulated and 179 downregulated in PP). Functional enrichment analysis highlighted enzymatic activity and immune response pathways. Notably, PP hens exhibited upregulation of *PNLIPRP1* ($\log_2$FC = 1.9, $p = 0.001$) and downregulation of *PLTP* ($\log_2$FC = −1.65, $p = 0.015$). Non-linear hierarchical approximation revealed a stochastic noise mode in DP ($\alpha = 45.05$, $p = 0.276$). Network analysis identified a compact regulatory cluster (*SFRP5*, *WNT5B*, *MMP13*) linked to the Wnt pathway. RT-qPCR validated RNA-Seq trends for five candidate genes; *SERPINB10B*, *MMP13* and *LYG3* expression increased 3.86- to 16.00-fold in DP ($p < 0.05$). These signatures offer potential candidate molecular markers for future exploratory breeding programs targeting extended egg-laying plateaus.

Check for updates

Academic Editors: Manuel García-Herreros and Pedro Manuel Aponte

Received: 22 September 2026
Revised: 23 October 2026
Accepted: 3 November 2026
Published: 6 November 2026

Copyright: © 2026 by the authors. Licensee MDPI, Basel, Switzerland. This article is an open access article distributed under the terms and conditions of the Creative Commons Attribution (CC BY) license.

Keywords: chicken (*Gallus gallus*); ovarian transcriptome; RNA-Seq; egg-laying plateau; laying persistence; egg production curve; Dekalb White laying hens; differential gene expression; stochastic noise; Wnt signaling pathway

1. Introduction

Maintaining and extending an active (including reproductive) lifespan is a priority in both human health [1] and agricultural systems such as poultry production [2]. For egg laying, the longevity of individual birds directly translates into economic factors in that early reproductive aging leads to an inefficient use of resources and subsequent high replacement costs of commercial egg production stocks [3,4]. Despite decades-long genetic improvement of egg-laying crosses [5–9], limited reproductive longevity [10] continues to impede progress, and it is thought that this may be a type of early physiological senescence of the reproductive system [11].

Important parameters for egg production, represented as an egg-laying curve [12,13], constitute the rate of egg laying, its peak [14,15] and the ability to maintain such a peak for consistently long periods [16,17]. Prolonging the egg-laying peak directly impacts profitability in that an increase in the number of eggs per hen reduces the costs of raising and replacing the flock [4]. From a market economics perspective, the technology of using chickens (*Gallus gallus*) for less than a year is ineffective compared to two or even three years [18]. Restricting commercial hens to a single short laying cycle fails to compensate for the substantial upfront and operational expenses, including feed, lighting, veterinary care and equipment depreciation. Furthermore, this practice necessitates frequent flock replacements, dramatically inflating pullet procurement costs and ultimately diminishing the overall profitability of the poultry enterprise. Modern chicken crosses can retain reserves for successful exploitation during the second and third egg-laying cycles [19] and it is thus essential to study the molecular mechanisms associated with individual reproductive cycle dynamics [20].

The duration of the peak egg-laying period (i.e., egg-laying curve plateau [21]) partly reflects the physiological resilience and reproductive longevity of birds [22]. Its reduction is often the result of accelerated depletion of the follicular reserve [23], imbalance in the hypothalamic–pituitary–gonadal axis [24], or progressive ovarian involution. This may be associated with chronic oxidative stress and inflammation [23]. An important aggravating factor in intensive production conditions is the chronic toxicological load caused by the presence of xenobiotics (mycotoxins, pesticide residues, and heavy metals) in feed [25–28]. Such toxins have been shown to induce oxidative stress [29–31], disrupt hormonal balance and trigger cell apoptosis [32], thereby accelerating the aging of the reproductive system [33].

In commercial poultry production, the problem of low performance after the first egg-laying cycle (“short cycle”) can be solved by forced, or induced, molting, which reboots the laying hen’s reproductive system [15]. This procedure, however, simultaneously creates several negative factors, i.e., a period of complete absence of egg production and increased risks of disease, mortality during the stressful period, and the subsequent animal welfare concerns that surround these practices [34]. An alternative solution is genetic selection for natural prolongation of the first production cycle, thereby potentially obviating the need for stressful manipulations [35]. Traditional methods based on phenotypic traits are often ineffective in predicting the reproductive potential of poultry, especially in the early stages of development [36]. Moreover, compared to intensive selection for production traits, significantly less attention is paid to the fertility of laying hens in breeding programs [36].

Given the above, it is essential to identify, and select for, genetic markers and specific candidate genes influencing aging and associated with reproductive longevity [15]. The use of such markers and genes will allow for more accurate and earlier selection of birds with high genetic potential [37–42]. Comparative transcriptome profiling using RNA sequencing (RNA-Seq) is a well-established tool to achieve this [43,44]. The aim of the study was, therefore, to conduct comparative transcriptome profiling of ovarian tissues from commercial hybrid layers of the Dekalb White (Hendrix Genetics BV, Boxmeer, The Netherlands) cross with contrasting egg production phenotypes—early and persistent plateau (PP) vs. late and degressive plateau (DP). Our working hypothesis was that hens exhibiting these divergent egg production curves differ not only across macroscopic zootechnical parameters but also display distinct ovarian transcriptomic realignments. Furthermore, we hypothesized that these localized transcriptional variations could serve as candidate molecular markers that potentially reflect individual reproductive longevity. The overarching purpose was to establish genetic factors that determine the physiological resource of egg productivity. Using RNA-Seq-assisted profiling of ovaries, we identified distinct differential expression patterns of important genes in hens with different stage-specific egg-laying plateau features.

2. Materials and Methods

2.1. Experimental Design and Formation of Experimental Groups

This study was conducted on a flock of Dekalb White egg-laying hens [45] at a research and production farm located in the village of Fyodorovskoye, Tosnensky District, Leningrad Oblast (Russia). The birds were provided by a private poultry farm located in the Leningrad Region. The transfer of the hens and the issuance of all required veterinary certificates were performed in strict compliance with the Law of the Russian Federation No. 4979-1 "On Veterinary Medicine" dated 14 May 1993 (as amended on 29 December 2025), ensuring full traceability of the birds' origin and transit. Prior to the experiment, all 120 hens were housed in a single facility in battery cages under controlled environmental conditions: ambient temperature of 18–20 °C, relative humidity of 60–70%, and a 16 h photoperiod. These housing standards adhered strictly to Order No. 188 of the Ministry of Agriculture of the Russian Federation dated 26 March 2025 "On Approval of Veterinary Rules for the Housing of Poultry for Breeding and Rearing Purposes". The animals were fed a nutritionally complete compound diet and had *ad libitum* access to water. Birds aged 20 weeks, free from pathologies and factors that could affect gene expression, were selected. The experiment continued until the birds reached 49.5 weeks of age. All animal care and experimental procedures were performed in strict accordance with the European Convention for the Protection of Vertebrate Animals used for Experimental and Other Scientific Purposes (ETS No. 123, Strasbourg, 1986) and the Russian Federation legislation on animal welfare, including Federal Law No. 498-FZ on Responsible Treatment of Animals. The hens were maintained under identical conditions, and the protocols for growing, housing, feeding, and handling complied with standard requirements described elsewhere (e.g., [46–51]). Specifically, the birds were fed a complete feed according to current nutrition regulations (Supplementary Table S1) and housed in individual cages. Light, temperature, and humidity regimes were maintained in strict accordance with the Dekalb White management guidelines [45].

At the preliminary stage, phenotypic stratification of the flock was carried out based on monitoring the dynamics of egg production traits (e.g., [52–55]). The separation criterion was the observed parameters of the egg-laying curve: the time to reach peak productivity and the duration of the plateau (i.e., stable period of high egg production), following the previously described method for analyzing cyclic patterns of productivity [21].

At the age of 49.5 weeks, two groups of hens (60 birds per cohort) with contrasting egg production curves were established. The first one was the PP (prolonged plateau) group characterized by an early-persistent production phenotype, i.e., layers that reached their peak egg-laying rapidly (at 24 weeks of age, which was 2–3 weeks earlier than the average) and maintained a high laying rate of ≥90% for more than 6 month, indirectly reflecting a high reproductive potential and resilience to reproductive aging. The second one was the DP (declining/degressive productivity) group characterized by a late-degraded production phenotype. These birds exhibited a delayed peak onset (at 27 weeks of age) and a transient, short-term productivity plateau lasting no more than 2 months. This was followed by a rapid decline in egg production by 10–15% or more, serving as an indirect indicator of accelerated reproductive senescence and compromised physiological resilience [21].

The selection of the 49.5-week age threshold for establishing the contrasting groups was based on two primary methodological considerations. First, by this time, all hens had fully completed the initial phase of egg-laying development and had surpassed their peak production. This allowed for an objective assessment of each bird's egg-laying curve, specifically regarding the timing of the peak onset and the overall duration of the productivity plateau. Second, at 49.5 weeks of age, hens with a short-lived plateau (the DP group) already exhibited a pronounced decline in productivity, whereas birds with a prolonged plateau (the PP group) maintained a consistently high laying rate. Sampling at this specific time point captured the maximum phenotypic contrast between the cohorts, which is crucial for identifying candidate genes linked to reproductive longevity.

To minimize random individual variation, a stringent selection process was applied in the subsequent stage. Out of the initial cohort of 60 birds per group, only three individuals per cohort exhibiting the most contrasting phenotypic traits were selected for RNA sequencing, with the individual bird serving as the experimental unit. This selection followed a predefined "extreme-phenotype contrast" paradigm rather than a random distribution. Specifically, individuals within the PP and DP cohorts were selected based on the duration of their individual egg-laying curves and associated zootechnical parameters (Supplementary Table S2).

In the PP group, the three selected hens demonstrated the most prolonged productive plateau within their 60-bird cohort, maintaining an intensity above 90% for over 6 months, alongside an early peak onset at week 23. Phenotypically, these PP birds exhibited the highest individual egg production (97.32%), the lowest body weight (1652.27 ± 26.19 g), a lower egg mass (57.13 ± 0.26 g), and the most efficient feed conversion ratio (1.489 kg per 10 eggs) within their cohort (Supplementary Table S2). Conversely, the three selected DP hens represented the shortest plateau within their respective 60-bird cohort, remaining above 90% for less than 2 months, with a delayed peak onset at week 28 followed by a rapid production decline. The DP phenotype was characterized by the lowest egg production (85.43%), a higher body weight (1869.05 ± 32.18 g), a higher egg mass (63.07 ± 0.22 g), and a poorer feed conversion ratio (1.569 kg per 10 eggs). Thus, the selected biological replicates reflected the most extreme, clear-cut representations of their respective phenotypes. Crucially, post-mortem veterinary necropsies confirmed that all selected individuals were clinically healthy, showing no signs of infectious or non-contagious pathologies that could alter the transcriptomic profiles.

This extreme-phenotype sampling design was intentionally employed to minimize background biological noise and maximize the probability of detecting true biological markers. At a cohort size of n = 3 per group, random sampling would predominantly capture baseline intra-group biological variability, thereby increasing the risk of a type II statistical error. Because the primary objective of this exploratory stage was to identify differentially expressed genes (DEGs) associated with the maintenance of the productive

plateau rather than to describe a generalized population average, this targeted approach is highly justified. While this sample size represents a widely accepted standard in exploratory transcriptomic studies [43,56], the direct comparison performed between these two phenotypically distinct groups remains a strategy specifically tailored to uncover candidate gene expression signatures linked to reproductive longevity.

2.2. Sampling

At the end of the study, the birds were euthanized using cervical dislocation that was performed without prior sedation. No chemical reagents or injectable anesthetics were administered before or during the euthanasia procedure, eliminating potential effects of reagents/anesthetics on gene expression profiles in tissues. This procedure was performed by qualified personnel in compliance with all bioethical standards to minimize stress and pain in the animals. Death of the bird was confirmed by cessation of heartbeat and respiration, absence of corneal and plantar reflexes, and complete muscle relaxation.

It should be noted that cervical dislocation without prior sedation represents a standard method of poultry euthanasia in experimental research and is widely approved by institutional ethics committees [57]. However, we acknowledge that this procedure can induce acute short-term stress. To suppress the potentially confounding effects of such stress on gene expression profiles, several rigorous standardization measures were implemented. For environmental and circadian control, all birds were euthanized at the same time of day in the same room to eliminate circadian and environmental variations. To ensure rapid sampling, the time interval between removing the bird from its cage and collecting the ovarian tissue sample was kept to a strict minimum. For operator consistency, the entire procedure was performed by the same highly experienced technician to ensure maximum technical uniformity. In terms of pre-experimental welfare, the hens were not subjected to feed withdrawal or any other external stressors for 24 h prior to euthanasia.

Ovarian tissue samples, specifically stroma fragments containing cortical follicles under 1 mm in diameter, were collected from the hens (n = 6, representing three individuals per group) for subsequent transcriptome analysis. To ensure the high quality required for downstream RNA-Seq, sampling was conducted under strict stereomicroscopic control without using histological fixatives or dyes, which can induce enzymatic and chemical degradation of RNA molecules [58]. The microdissection was performed under a binocular stereomicroscope (MS-6-ZOOM LED; OOO Nablyudatelnye Pribory, St. Petersburg, Russia) at up to 40× magnification using ophthalmic scissors with ultra-sharp microblades. This approach ensured precise microsurgical dissection with minimal mechanical cell damage. To warrant sample homogeneity, each specimen was evaluated against the following anatomical parameters: (1) visual uniformity (consistent tissue coloration without signs of hyperemia or ischemia); (2) absence of lipophilic inclusions (no yellowish inclusions indicative of yolk sac remnants); (3) structural consistency (uniform tissue texture lacking visible indurations or nodules); and (4) exclusion of extraneous structures. The latter implied complete absence of blood vessels or fragments of larger follicles exceeding 1 mm in diameter. Any samples exhibiting signs of heterogeneity were immediately discarded and replaced with compliant tissue specimens. This tailored protocol closely follows established methodological frameworks for avian ovarian transcriptomics, where pre-isolation histological staining is strictly omitted [59].

The ovarian stroma containing cortical follicles under 1 mm in diameter was specifically selected for transcriptome analysis based on several key biological considerations. To achieve functional significance, small follicles (<1 mm) represent the most critical ovarian fraction, as they constitute the pool of activating follicles from which future eggs develop [60]. To observe cellular composition, this tissue encompasses vital cellular compo-

nents, namely oocytes and granulosa cells, which are directly involved in folliculogenesis, steroidogenesis, and the overarching regulation of reproductive function [61]. To secure baseline stability, the stroma with small cortical follicles, unlike larger, preovulatory follicles, is less susceptible to the immediate physiological fluctuations of the ovulatory cycle, thereby allowing for an accurate assessment of the fundamental molecular mechanisms underlying long-term reproductive potential [62].

Samples were collected using an aseptic technique and immediately placed in IntactRNA solution (Eurogen, Moscow, Russia). The samples were then promptly delivered to the BIOTROF+ laboratory (Fyodorovskoye, Tosnensky District, Leningrad Oblast, Russia), where they were first incubated at 4 °C for 24 h to allow thorough reagent penetration, and subsequently frozen at −20 °C. The frozen tissues were maintained at −20 °C for a standardized duration of 10 days prior to total RNA extraction and subsequent sequencing. This specific 10-day storage interval was strategically implemented to await the comprehensive results of the systemic blood analyses, ensuring that all chosen replicates strictly conformed to the physiological health inclusion criteria before initiating high-throughput processing. Crucially, this storage duration and all environmental conditions were strictly identical for all samples across both experimental groups. This absolute procedural uniformity effectively eliminates any confounding systematic errors or processing biases related to differential RNA degradation.

2.3. Necropsy and Hematological Analysis of Poultry

Necropsy of internal organs was performed according to generally accepted methodologies for avian post-mortem examination [63]. This evaluation comprised two distinct phases. First, a broad pathological screening of 15 birds per cohort was conducted to exclude subclinical conditions that could confound the transcriptomic data. Second, detailed organ morphometric measurements were taken strictly from the subset of three hens per group (n = 3) designated for subsequent ovarian RNA sequencing.

Prior to dissection, an external examination of the carcass was conducted to evaluate the condition of the plumage, visible mucous membranes, skin integument, and the presence of any pathological discharges. The carcass was secured in a dorsal recumbent position on a dissection table, with the wings and limbs pinned. The abdominal wall was opened via a longitudinal midline incision extending from the cloaca to the sternum, followed by skin reflection to expose the thoracic and abdominal cavities. Using bone shears, bilateral incisions were made through the ribs along both sides of the sternum parallel to the keel, the pectoral muscles and ribs were transected, and the peritoneum was opened.

Following this systemic pathological clearance, detailed morphometric measurements of the internal organs were recorded exclusively for the three individuals per group selected for sequencing (reflected in Supplementary Table S3). Restricting these precise morphometric profiles to the exact biological replicates used for ovarian tissue microdissection ensured direct, unconfounded correlation between organ phenotypes and the high-throughput transcriptomic datasets.

Blood samples were collected from the wing vein (vena cutanea ulnaris) of the laying hens from both groups (n = 3 per group), utilizing the exact same individual birds designated for the ovarian microdissection and transcriptomic sequencing. Vacuum tubes containing EDTA were used for hematological assays, while tubes with a clot activator were employed for serum isolation. Following established protocols [64], red blood cell (RBC) and white blood cell counts were evaluated using a Goryayev hemocytometer. Differential leukocyte counts (leukograms) were determined microscopically on blood smears stained with May–Grünwald fixative and Romanowsky–Giemsa stain. Hemoglobin levels were measured via the hemiglobincyanide method, and packed cell volume (PCV, or

hematocrit) was determined by centrifugation. This aligned sampling framework ensured a direct correlation between systemic physiological indices and localized ovarian gene expression signatures.

Immunoglobulin classes were quantified using the discrete precipitation method described by Kostyna [64,65]. Immunological profiles included the determination of serum bactericidal activity (SBA), serum lysozyme activity, concentrations of immunoglobulins A, M, and G (IgG), alongside phagocytic metrics (phagocytic index and phagocytic number) [66]. Biochemical parameters, encompassing total calcium, inorganic phosphorus, potassium, sodium, iron, total protein, uric acid, creatinine, bilirubin concentrations, and the enzymatic activities of amylase, alkaline phosphatase (ALP), alanine aminotransferase, and aspartate aminotransferase, were determined using commercial kits from Abris+ LLC (St. Petersburg, Russia) on a ChemWell automated analyzer (Awareness Technology, Palm City, FL, USA).

2.4. RNA-Seq, Sequence Processing and Bioinformatic Data Analysis

Total RNA was isolated from ovarian tissue using the Aurum™ Total RNA Mini Kit (Bio-Rad, Hercules, CA, USA). The purity and concentration of the obtained RNA were verified spectrophotometrically using a NanoDrop 2000 instrument (Thermo Fisher Scientific, Wilmington, DE, USA). The optical density (A260/A280) was in the range of 1.8–2.1, confirming a high degree of sample purification from impurities. RNA integrity was determined on an Agilent Bioanalyzer 2100 system using the RNA Nano 6000 kit (Agilent Technologies, Santa Clara, CA, USA). Finally, cDNA was prepared using iScript™ Reverse Transcription Supermix (Bio-Rad).

To construct sequence libraries, we used the commercial TruSeq® Stranded mRNA LT (Set A) kit (Illumina, San Diego, CA, USA), following the manufacturer's protocol. Sequencing of the libraries was performed on the Illumina MiSeq platform using the MiSeq® Reagent Kit v3 (150 cycles), with the read length being 115 bp.

Using the relevant bioinformatics tools that we had previously tested and implemented in related investigations [67–72], the generated RNA-Seq data were successively processed in silico. In particular, primary processing of raw reads was performed using FastQC (version 0.12.1; https://www.bioinformatics.babraham.ac.uk/projects/fastqc; accessed on 21 September 2026) and multiQC (version 1.33; [73]) software. Subsequent bioinformatics analysis included quality control steps, adapter sequence trimming, and low-quality read filtering using Trimmomatic (version 0.39; [74]). Construction of the genome reference index and primary data alignment were performed using HISAT2 (version 2.0.5; [75]). Filtered read alignment was performed on the chicken sequence assembly bGalGal1.mat.broiler.GRCg7b (Ensembl release 108; https://www.ncbi.nlm.nih.gov/datasets/genome/GCF_016699485.2/; accessed on 21 September 2026) that was also used as a reference genome in our other works [70,76,77].

For precise splicing accounting and quantitative assessment of gene expression, the RSEM package (version 1.3.3; https://deweylab.github.io/RSEM/; accessed on 21 September 2026) with the built-in STAR (Spliced Transcripts Alignment to a Reference; [78]) algorithm was used. Calculations were performed in multi-threaded mode using the full-length DNA sequence (toplevel).

2.5. Differential Gene Expression (DGE) Analysis

To ensure objectivity and eliminate potential bias, a strict blinding procedure was maintained during data processing: the co-authors responsible for the bioinformatic and statistical analyses were completely blinded to the phenotypic group assignments of the individual samples. Statistical analysis of DEGs was performed in R (version 4.5.2; https:

//www.R-project.org/; accessed on 21 September 2026) using the DESeq2 package (version 1.50.2; [79]). The initial gene-level expected count matrix was generated from the raw sequencing outputs utilizing the rsem-generate-data-matrix script from the RSEM pipeline (https://github.com/deweylab/RSEM/blob/master/rsem-generate-data-matrix; accessed on 21 September 2026). This processing step yielded a total of 30,108 loci, which were subsequently converted to the nearest integers using the native R base round() function (https://www.rdocumentation.org/packages/base/versions/3.6.2/topics/Round; accessed on 21 September 2026) to ensure full downstream compatibility with DESeq2's parametric modeling requirements. At the preprocessing stage, preliminary filtering was performed: genes with a total read count of less than 10 across all samples were excluded, which allowed us to form a working set of 17,285 of the most informative loci. To correctly compare samples with different sequencing depths and library compositions, internal data normalization was performed using the median-of-ratios method built into the DESeq2 algorithm [79].

To assess biological variability between groups and verify data quality, principal component analysis (PCA) of transcriptome profiles was performed using the 500 most variable genes. The PCA plots were built using the respective tool the in the Phantasus web service (version 1.31.1; [80]). Differences between groups were assessed using generalized linear models [81]. The lfcShrink algorithm (apeglm method; [82]) was used to stabilize logarithmic expression change estimates. Genes were considered significant at adjusted p-value (p-adj) < 0.05 according to the Benjamini–Hochberg correction [79]. DESeq2 results were visualized by constructing Volcano plots using the ggplot2 package (version 4.0.1; https://cran.r-project.org/web/packages/ggplot2/index.html; accessed on 21 September 2026).

Gene functional annotation and gene ontology (GO) enrichment analysis were performed using the KEGG database (https://www.genome.jp/kegg/; accessed on 21 September 2026). To identify biological trends, gene set enrichment analysis (GSEA) was performed on a pre-selected set of significant DEGs at $p < 0.05$ and modulus of $\log_2$ fold change $|\log_2 FC| \geq 1$ [83]. Additionally, GSEA was applied to the full ranked list of genes sorted by descending $\log_2 FC$ values to systematically assess functional shifts. The functional enrichment plot for GO analysis was built using the dotplot function from the graphics package (version 4.2.3; [84]). The heatmap graphs showing the complete transcriptome profile, i.e., expression of all genes and transcripts, in ovarian tissues of laying hens with different modes of reproductive longevity were constructed using the Phantasus web service. In this case, the ranking and ordering of elements on the axes was carried out based on the metrics of the GSEA algorithm. The normalized enrichment score (NES) was used as a quantitative criterion and a direction indicator of expression changes [85]. A complete set of pre-filtered array of genetic determinants was used for construction.

To minimize the risk of a Type II error and ensure sufficient statistical power, two sequential significance thresholds were applied at different stages of the analysis [86]. At the preliminary stage, an unadjusted p-value threshold ($p < 0.05$) was utilized to screen a broad pool of 484 genes, allowing for an evaluation of the global transcriptomic architecture. Concurrently, to model the non-linear hierarchical/fractal approximation and identify single key signals, a more stringent statistical criterion was implemented using the Benjamini–Hochberg false discovery rate correction (p-adj < 0.05 and $|\log_2 FC| \geq 1$) [79].

To visualize the functional relationships between the identified DEGs and reveal key regulatory nodes, a protein–protein interaction network analysis was performed. The interaction network was constructed using the STRING database (version 12.0) via the stringApp plugin (version 2.2.0; [87]) in the Cytoscape environment (version 3.10; [88]). The input data included 116 genes encoding characterized proteins for *G. gallus*. Both direct

physical interactions and functional associations were considered to form connections. The confidence score threshold was set at 0.400. The final graph visualization was performed using the Files Orthogonal Layout algorithm (version 1.2; [88]). For visual data analysis, $\log_2$FC and *p*-values were imported into the network. Hub genes were identified using the *cytoHubba* plugin [89]. Gene ranking was performed using the Maximum Clique Centrality (MCC) algorithm that is the most effective for finding dense functional clusters in biological networks [90].

To ensure the robustness of the conclusions and account for potential model dependence, the systemic stability of the transcriptome response was analyzed using independent mathematical approximations. Calculations were performed for a functional core comprising 16 key genetic determinants selected from the general list of DEGs at a significance threshold of p-adj < 0.05. To assess the nonlinear hierarchical determination of the system, an additive-exponential model (1) was employed using the formula [91]:

$$NC(N) = \alpha + K \times e^N, \quad (1)$$

where *NC* is the normalized absolute level of gene expression (based on *normalized counts* from DESeq2); *N* is the ordinal number (rank) of a gene in the series of increasing absolute deviation; *K* is the amplitude of the regulatory response, i.e., a reflection of the intensity of the coordinated expression of key genetic determinants over the baseline level α of stochastic noise (network integration); and *e* is the Euler number (i.e., the base of the natural logarithm).

Additional normalization of the initial data to the modulus and shift in the scale to zero were not carried out, since the values used (normalized counts) are proportionate positive quantities, the calculation of which initially starts from natural zero.

The model parameters (α, K) were estimated using the nonlinear least squares method [92]. All calculations were implemented in the R environment (version 4.5.2). The quality of the approximation was assessed by the coefficient of determination (R^2).

2.6. Quantitative Real-Time PCR (RT-qPCR)

To validate the reliability of the high-throughput RNA-Seq dataset, seven key candidate genes representing diverse functional biological categories and demonstrating robust differential expression profiles were selected for RT-qPCR verification (Table 1).

The specific oligonucleotide primers (Table 1) were dynamically designed using the NCBI Primer-BLAST tool (https://www.ncbi.nlm.nih.gov/tools/primer-blast/; accessed on 21 September 2026). The actin beta (*ACTB*) gene was selected as the internal reference standard for target gene normalization.

Amplification was performed using a DTlite real-time PCR cycler (DNA-Technology, Moscow, Russia) and the SsoAdvanced™ Universal SYBR® Green Supermix (Bio-Rad, Hercules, CA, USA) in strict accordance with the manufacturer's operational protocols [93]. The thermal cycling parameters were optimized as follows: initial denaturation at 95 °C for 5 min, followed by 40 cycles of denaturation at 95 °C for 30 s, annealing at 60 °C for 30 s, and extension at 70 °C for 30 s [94]. All assays were conducted in technical triplicate utilizing the identical RNA sample aliquots deployed for the initial RNA-Seq libraries. Relative gene expression folds were calculated using the comparative $2^{-\Delta\Delta CT}$ method [95].

Table 1. Oligonucleotide primer sequences used for RT-qPCR validation of differentially expressed genes identified by ovarian transcriptomic analysis in Dekalb White hens.

Gene Symbol	Protein/Gene Name	Forward (F) and Reverse (R) Primer Sequences (5′–3′)
ID2	inhibitor of DNA binding 2, HLH protein	F: CCTTTCGGAGCACAACCT R: GAGCGCTTTGCTGTCACTC
MMP13	matrix metalloproteinase-13 (collagenase 3)	F: TTTGGATTAGAGGTGACGG R: CCACTTCGTATTCTGGTGA
AvBD4	avian beta-defensin 4	F: TCATGGAGCTGTGGGCTTTT R: AGCATTCCCATAAGGGCATT
SERPINB10B	serpin peptidase inhibitor, clade B (ovalbumin), member 10 B	F: AACCCTTCCGACTGAGCAAG R: ATCAGCCCATTCTGACAGCC
SFRP5	secreted frizzled related protein 5	F: CCTGTCATGGAGTCCTA CGGCT R: ATCATGCCATCCG CCTTGTG
HSPB9	heat shock protein family B (small) member 9	F: CACAACGCTCCCAACTCC R: CGATGCAGACCGTTGTTCC
LYG3	lysozyme g3	F: TTGCTACGGCAGTGTAAGCA R: ACCAAGGTTGGAAAGACCCA
ACTB	actin beta	F: CTGTGCCCATCTATGAAGGCTA R: ATTTCTCTCTCGGCTGTGGTG

2.7. Statistical Analysis of Performance Indicators

Mathematical and statistical processing of layer performance data was performed using multivariate analysis of variance (ANOVA) in Microsoft Excel XP/2003 and the RStudio environment (version 2025.9.2.418; http://www.posit.co/; accessed on 21 September 2026). The results were presented as the mean (M) and standard error of the mean (± SEM). The statistical significance of differences was determined using Student's *t*-test, with differences being considered significant at $p < 0.05$. For pairwise comparison of mean values, the Tukey HSD test was applied using the TukeyHSD function from the R Stats package (https://search.r-project.org/R/refmans/stats/html/TukeyHSD.html; accessed on 21 September 2026).

3. Results

3.1. Zootechnical Performance, Morphometric Evaluation of Internal Organs, and Hematological Profiles

To establish a robust and contrastive experimental design for subsequent RNA sequencing and maximize the possibility of identification of differentially expressed genes, six individuals exhibiting the most extreme phenotypic traits ($n = 3$ per group) were selectively sampled from an initial production cohort of 60 birds per group. The definitive inclusion criteria for this finalized subset ($n = 3$ per group) within the early-persistent production (PP) group, directly contrasted against the three selected individuals from the late-degraded production (DP) group, comprised an accelerated onset of the egg-laying plateau (24 vs. 27 weeks), a superior average egg production rate (97.32% vs. 85.43%), and a significantly lower body weight (1652.27 ± 26.19 g vs. 1869.05 ± 32.18 g; $p < 0.05$); Supplementary Table S2).

Subsequent morphometric post-mortem analysis revealed distinct organosomatic shifts between the two performance phenotypes (Supplementary Table S3). The DP hens were characterized by a significantly higher liver weight (44.55 ± 1.10 g vs. 34.85 ± 2.55 g in the PP group; $p < 0.05$) alongside an 11.4% increase in abdominal fat accumulation ($p < 0.05$). Spleen and oviduct weights in the DP group were also elevated, showing an

increase of 28.7% (from 1.74 ± 0.16 g to 2.24 ± 0.35 g) and 13.0 g ($p < 0.05$), respectively, although oviduct length was slightly reduced ($p < 0.05$). Conversely, secondary sexual characteristics in the DP group were less pronounced, as evidenced by a marked reduction in both comb weight (decreasing from 22.89 ± 1.31 g to 17.32 ± 1.51 g; $p < 0.05$) and comb length ($p < 0.05$).

Regarding the systemic physiological status, all evaluated clinical, hematological, and biochemical blood parameters for both groups remained strictly within the standard physiological reference ranges for poultry [96] (Supplementary Tables S4–S7). Nevertheless, fine-grained variations between the phenotypes were observed. Specifically, the DP group displayed slight but statistically significant reductions in red blood cell count, hemoglobin levels, and blood color index values ($p < 0.05$), whereas its PCV was increased by 4.67% compared to the PP group ($p < 0.05$). Immunological profiling further indicated altered metabolic and defense responses in the lower-performing phenotype. The DP hens exhibited a 7.1% increase in SBA and an elevation of IgG by 2.36 g/L ($p < 0.05$; Supplementary Table S5). These shifts were accompanied by a significant drop in total protein and β-globulin concentrations—decreasing by 17.7 g/L and 3.9%, respectively ($p < 0.05$; Supplementary Table S6)—while ALP activity demonstrated a 1.3-fold upregulation compared to the high-performing PP counterparts ($p < 0.05$; Supplementary Table S7).

3.2. RNA-Seq Data Quality and Mapping Statistics

As a result of mapping RNA-Seq reads to the reference genome, a transcriptomic profile of laying hen ovarian tissues was determined for a total of six samples, comprising, on average, 41.46 (± 9.0) × 10^6 high-quality reads (i.e., clean reads) for each sample. The proportion of nucleotides with an accuracy level of Q25 (with error probability ≤ 0.32%) exceeded 99.9%, and the proportion of nucleotides with an accuracy level of Q30 (with error probability ≤ 0.1%) was at least 97.5% for all libraries (Table 2).

Table 2. Statistics of data quality [1], mapping, and transcriptome expression assessment based on RNA-Seq data from ovarian tissues of Dekalb White laying hens from the PP and DP groups.

Sample	Clean Reads	Clean Nucleotides, bp	Q25, %	Q30, %	GC, %	Total Mapped (%)	Uniquely Mapped (%)	Mapped to Multiple Positions (%)
PP group								
1	47,107,838	10.84×10^9	100.0	98.8	46.0	43,669,863 (92.71)	42,132,260 (89.44)	1,491,185 (3.17)
2	44,897,757	10.84×10^9	100.0	98.9	45.0	41,051,898 (91.43)	39,603,264 (88.21)	1,448,634 (3.22)
3	52,210,281	12.01×10^9	100.0	98.9	46.0	47,737,109 (91.44)	46,026,742 (88.16)	1,710,367 (3.28)
DP group								
1	32,021,617	7.36×10^9	100.0	97.5	46.0	29,935,834 (93.49)	28,739,943 (89.75)	1,195,891 (3.74)
2	27,953,408	6.43×10^9	100.0	98.4	45.0	25,876,303 (92.57)	24,956,234 (89.28)	920,069 (3.29)
3	44,590,944	10.26×10^9	100.0	98.6	46.0	40,927,315 (91.78)	39,504,303 (88.59)	1,423,012 (3.19)

[1] Q25/Q30, proportion of nucleotides with sequencing accuracy of 99.68% and 99.90%, respectively; GC, percentage of guanine (G) and cytosine (C) in the array of cleaned reads (i.e., clean data).

During the subsequent expression analysis, clean reads were mapped to the current assembly of the *G. gallus* GRCg7b reference genome. The average percentage of successfully mapped reads (i.e., total mapped) was 92.24% of the total dataset (Table 2). Most of these reads (88.16–89.75%) were uniquely mapped. The percentage of reads mapped to multiple positions (i.e., multiple mapped) ranged from 3.15% to 3.74%. The guanine and cytosine (GC) content in the libraries ranged from 45% to 46%.

3.3. Transcriptome Profile of Hens with PP vs. DP of Egg Production

All samples demonstrated a clear separation into two clusters that corresponded to the PP and DP groups (Figure 1). The first principal component (PC1) explained 64.9% of the total data variance. The second component (PC2) accounted for 14.3% of the variance.

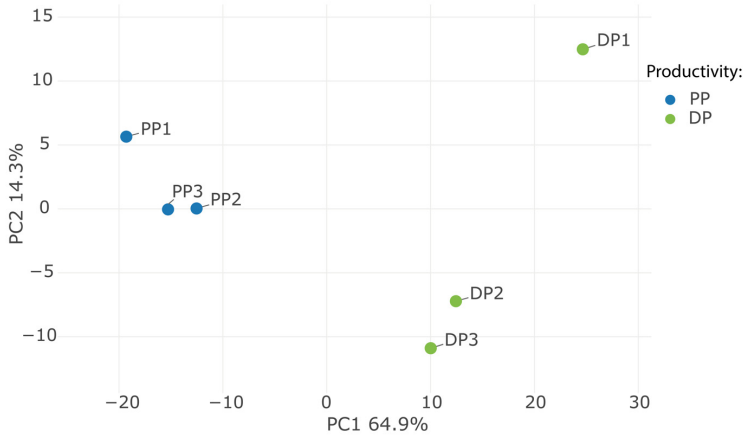


Figure 1. Principal component analysis plot for ovarian tissue transcriptome data. Visualization of biological variability between PP (blue) and DP (green) layer groups.

Global rank distribution analysis of the total transcriptome performed using the GSEA algorithm (for 17,285 genetic determinants) did not result in an overall statistically significant difference between the study groups (NES = −1.00; p = 0.49; Figure 2).

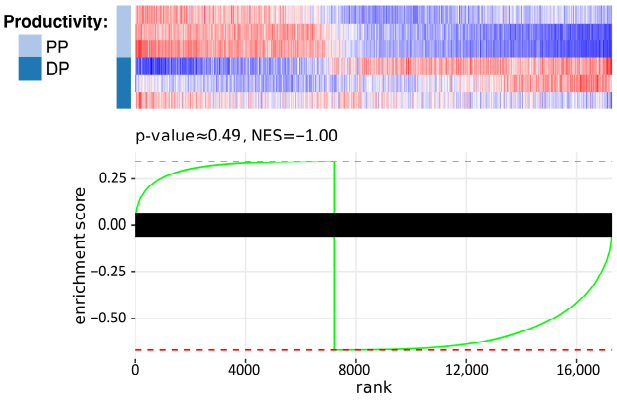


Figure 2. Heatmap and distribution of rank metrics of the whole transcriptome (17,285 expressed genes) in ovarian tissues of laying hens with different levels of reproductive longevity obtained using the GSEA algorithm. The color scale on the top plot reflects the expression level, with red corresponding to upregulation and blue to downregulation. Genes are ranked by the magnitude of differential expression between the PP and DP groups. Genes with maximum expression in the PP group are located at the top (or left) of the graph, and genes with maximum expression in the DP group are located at the opposite. In the lower plot, the y-axis values conform to the enrichment score, and those of the x-axis to a ranked list of all genes sorted by their differential expression between the two groups. Genes with the highest expression in the PP group are located on the left, and genes with the highest expression in the DP group are located on the right. The null hypothesis thresholds are indicated by red dashed lines. The solid green line represents the dynamics of the accumulation of differences between the groups. The area, composed of vertical thin gray lines, displays the positions of genes as a continuous, ranked list, where each individual gene is represented by a line.

Using the standard pretest criteria ($|\log_2 FC| \geq 1$ and unadjusted p-value < 0.05), we identified a wide range of potential changes for 484 genes, including 305 upregulated and 179 downregulated ones in the PP group relative to DP (Figure 3).

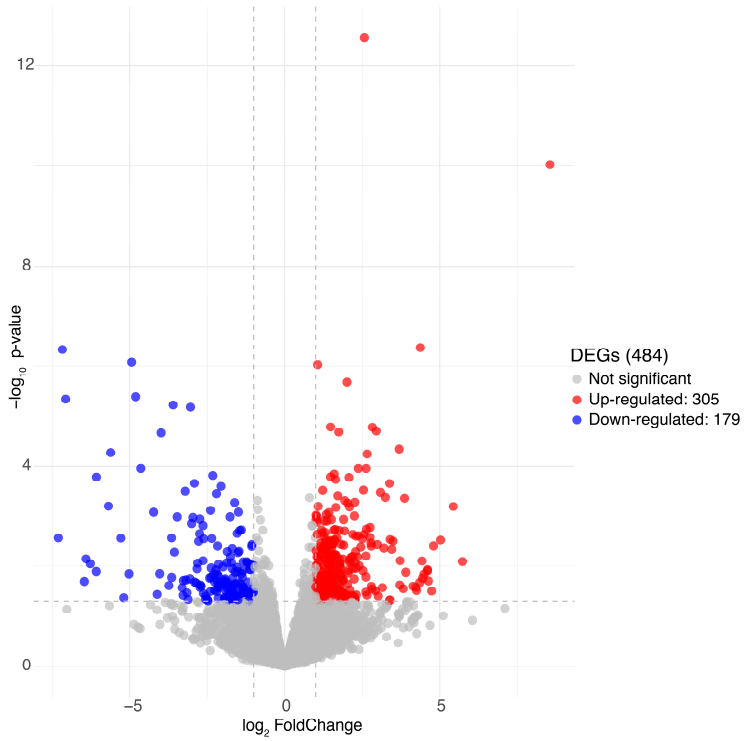


Figure 3. Volcano plot (scatterplot) showing genes in ovarian tissues that differ in expression level between the PP and DP groups of layers and reflecting the distribution of all genes (at $p < 0.05$). The x-axis represents the $\log_2$ fold change ($\log_2$FC), i.e., the logarithm of the gene expression ratio in the PP group compared to the DP group. The y-axis represents $-\log_{10}$ p-value that indicates the statistical significance of differences in expression and converts low p-values into large positive numbers to facilitate visualization. Each point on the graph corresponds to one gene. Genes with a p-value less than the threshold and an absolute $\log_2$FC value greater than the threshold are considered significantly differentially expressed and are highlighted in red and blue. Genes whose expression changes are not statistically significant are shown in gray. On the right side, the dots conform to upregulated genes in the PP group, and the dots on the left side to upregulated genes in the DP group. The horizontal dashed line represents the threshold for statistical significance ($p < 0.05$), while the vertical lines represent the threshold for the magnitude of expression change ($|\log_2\text{FC}| \geq 1$).

3.4. KEGG Pathway and GO Enrichment Analyses

The results of the analyses of the biological functions and key regulatory mechanisms of DEGs in ovarian tissue using the KEGG and GO databases allowed us to associate genes with signaling pathways. Both the specificity of the functional analysis and the identification of the most reliable biological functionality patterns were improved for a set of significant DEGs using GSEA. In particular, 11 of the most significant categories were detected, including enzymatic activity (lipase and carboxylester hydrolase), carbohydrate metabolism, and immune response. Changes in fundamental GO categories, such as molecular functions and their regulation, were also revealed (Figure 4). In the PP group, an increase in the lipase activity associated with the *PNLIPRP1* (pancreatic lipase related protein 1) gene was found compared to the DP group ($\log_2$FC = 1.9, $p = 0.001$). At the same time, downregulation of the *PLTP* (phospholipid transfer protein) gene was noted in the PP group compared to the DP group ($\log_2$FC = −1.65, $p = 0.015$).

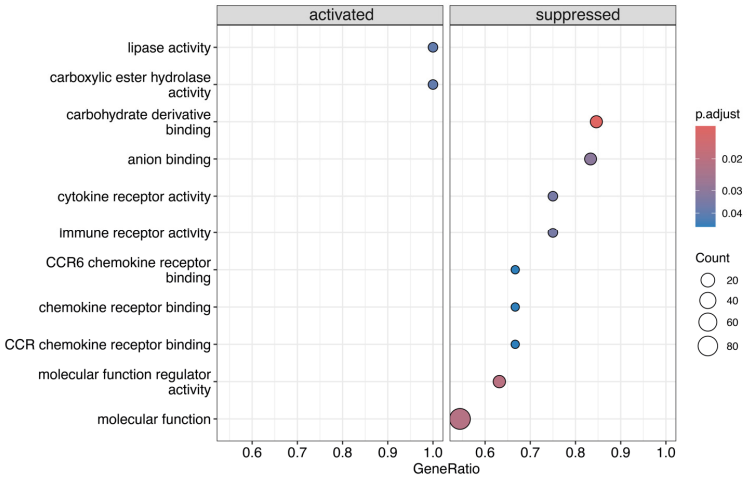


Figure 4. Gene ontology functional enrichment of DEGs within the molecular function category in follicle tissues of PP and DP laying hens. The enrichment diagram (dotplot) shows the ratio of gene counts on the *x*-axis; the dot size corresponds to the number of significant genes, and the color scale indicates the significance level. The analysis was performed using GSEA on a set of significant genes ($p < 0.05$).

Using GSEA on the complete transcriptome dataset, the prevalence of molecular processes associated with the activity of chemokine and cytokine receptors, as well as lipopolysaccharide binding, was revealed (Supplementary Figure S1). For example, a significant upregulation of the *CPLX1* (complexin 1) gene was detected in the ovary tissues of high-producing birds from the PP group ($\log_2$FC = 1.5, $p = 0.005$). Expression of the *AvBD4* (avian beta-defensin 4) gene in the ovary of DP chickens was 48 times greater than in PP hens ($\log_2$FC = −5.62, $p = 0.0001$, p-adj = 0.058). In addition, an abrupt 6.2-fold induction of the *HSPB9* (heat shock protein family B (small) member 9) gene expression was detected in PP chickens ($\log_2$FC = 2.62, $p = 0.0001$, p-adj = 0.099).

3.5. Network Analysis of Protein–Protein Interactions and Expression of Significant DEGs

Our network analysis using the MCC algorithm revealed a group of highly connected hub genes (Figure 5): *TLR4* (toll like receptor 4; score = 246, degree = 17), *CCR2* (C-C motif chemokine receptor 2; score = 235, degree = 12), *TLR7* (toll like receptor 7; score = 223, degree = 10), *TLR2A* (toll like receptor 2A; score = 168, degree = 9), *LY86* (lymphocyte antigen 86; score = 150, degree = 7), and *TLR1A* (toll like receptor 16; score = 144, degree = 6).

Furthermore, the network analysis identified a compact and significant (at p-adj < 0.05) regulatory cluster, including the *SFRP5* (secreted frizzled related protein 5), *WNT5B* (Wnt family member 5B) and *MMP13* (matrix metalloproteinase 13) genes (Figure 5). This cluster also embraces the genes *MMP10* (matrix metallopeptidase 10) and *IHH* (Indian hedgehog). Although there were significant p-values for these two genes (0.01 and 0.03, respectively), they had insignificant p-adj values (> 0.05) and lower $|\log_2\text{FC}|$ values: 1.00 and −2.1 for *IHH*, and 0.97 and −1.7 for *MMP10*, respectively. Despite a relatively small number of internal connections, this cluster is functionally integrated into the overall transcriptome network through the central *ALB* (albumin) node.

Overall, the application of more stringent statistical significance criteria (p-adj < 0.05 and $|\log_2\text{FC}| \geq 1$) allowed us to identify 16 of the most significant DEGs, including nine upregulated genes and seven downregulated genes in the PP group compared to DP hens (Figure 6, Table 3).

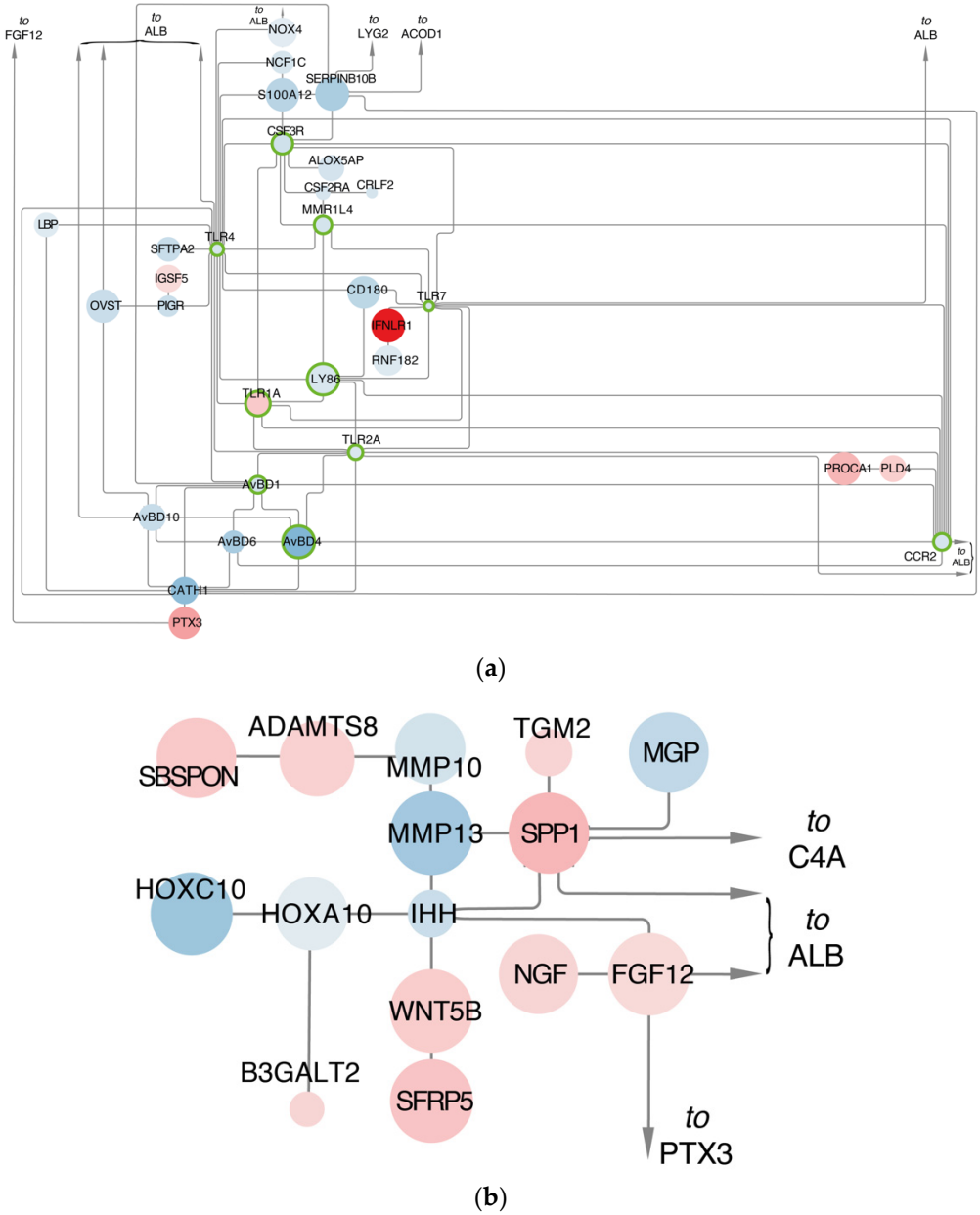


Figure 5. Network analysis of protein–protein interactions of differentially expressed genes in chicken follicle tissues. The network was constructed for 116 genes encoding characterized proteins for *G. gallus*. (**a**) The top 10 highly connected hub genes (highlighted by a green contour line); (**b**) the regulatory cluster, including the *SFRP5* (secreted frizzled related protein 5), *WNT5B* (Wnt family member 5B) and *MMP13* (matrix metalloproteinase 13) genes (at p-adj < 0.05). The lines indicate the presence of functional and physical associations between proteins. The color of the nodes reflects the direction of expression changes: red, upregulation; blue, downregulation. The diameter of the nodes is proportional to the significance level (based on p-values): large nodes correspond to the most significant changes (e.g., *FGF12* (fibroblast growth factor 12), $p = 0.001$). The full version of the network is presented in Supplementary Figure S2.

Some genes in this list currently lack detailed functional annotations in available Ensembl and National Center for Biotechnology Information (NCBI) databases. However, most DEGs (*SLC13A1*, *ID2*, *MMP13*, *SERPINB10B*, *PDCL2*, *WNT5B*, *LYG3*, *IFNLR1*, *SFRP5*, *FHAD1*, *LOC121106470*, etc.) were represented by genes with known functional annotations (Table 3).

Table 3. Genes showing the most significant differences in upregulation (up) or downregulation (down) levels (M ± SEM) [1] between the PP and DP laying hens. Values are expressed as normalized read counts, assuming p-adj < 0.05 and $|\log_2 FC| \geq 1$.

Ensembl Gene ID	Gene Symbol	Gene Name	PP Group	DP Group	p-Value	p-adj	$\log_2$FC	Regulation Type	Chromosome
ENSGALG00010001714	*SLC13A1*	solute carrier family 13 member 1	79.19 ± 8.50	19.57 ± 3.96	2.1×10^{-6}	0.006	2.01	up	1
ENSGALG00010003117	*ID2*	inhibitor of DNA binding 2, HLH protein	1438.93 ± 103.29	690.31 ± 19.63	9.4×10^{-7}	0.003	1.06	up	3
ENSGALG00010003124	lncRNA	predicted gene	55.00 ± 14.46	7.78 ± 3.35	1.7×10^{-5}	0.025	2.82	up	6
ENSGALG00010003609	*RNA18S11*	RNA, 18S ribosomal 11	1.37 ± 1.68	42.30 ± 10.30	8.4×10^{-7}	0.003	−4.94	down	16
ENSGALG00010007330	*MMP13*	matrix metalloproteinase-13 (collagenase 3)	12.09 ± 0.37	192.03 ± 149.18	2.2×10^{-5}	0.027	−3.99	down	1
ENSGALG00010008980	Non-annotated	predicted gene	0	20.36 ± 11.59	4.5×10^{-6}	0.010	−7.07	down	Z
ENSGALG00010011664	*SERPINB10B*	serpin peptidase inhibitor, clade B (ovalbumin), member 10 B	39.66 ± 9.92	480.36 ± 350.71	6.0×10^{-6}	0.012	−3.60	down	2
ENSGALG00010011783	lncRNA	predicted gene	36.48 ± 8.56	4.77 ± 1.66	2.0×10^{-5}	0.027	2.95	up	4
ENSGALG00010013321	*PDCL2*	phosducin like 2	18.04 ± 6.49	148.21 ± 75.33	6.6×10^{-6}	0.012	−3.04	down	4
ENSGALG00010013899	*WNT5B*	Wnt family member 5B	175.52 ± 16.82	62.61 ± 11.69	1.7×10^{-5}	0.025	1.48	up	1
ENSGALG00010015831	*LYG3*	lysozyme g3	34.96 ± 20.81	978.30 ± 1008.52	4.0×10^{-6}	0.010	−4.81	down	1
ENSGALG00010015838	*IFNLR1*	interferon lambda receptor 1	81.65 ± 28.86	0.00 ± 0.00	9.4×10^{-11}	9.2×10^{-7}	8.56	up	23
ENSGALG00010017808	*SFRP5*	secreted frizzled related protein 5	243.65 ± 30.37	73.31 ± 20.20	2.1×10^{-5}	0.027	1.74	up	6
ENSGALG00010020709	lncRNA	predicted gene	0.29 ± 0.36	42.74 ± 18.79	4.7×10^{-7}	0.002	−7.17	down	10
ENSGALG00010020955	*FHAD1*	forkhead associated phosphopeptide binding domain 1	200.16 ± 26.50	33.52 ± 4.00	2.8×10^{-13}	5.4×10^{-9}	2.57	up	21
ENSGALG00010028062	*LOC121106470*	deaminated glutathione amidase-like	269.46 ± 69.18	12.70 ± 10.79	4.3×10^{-7}	0.002	4.37	up	25

[1] M, mean; SEM, standard error of the mean.

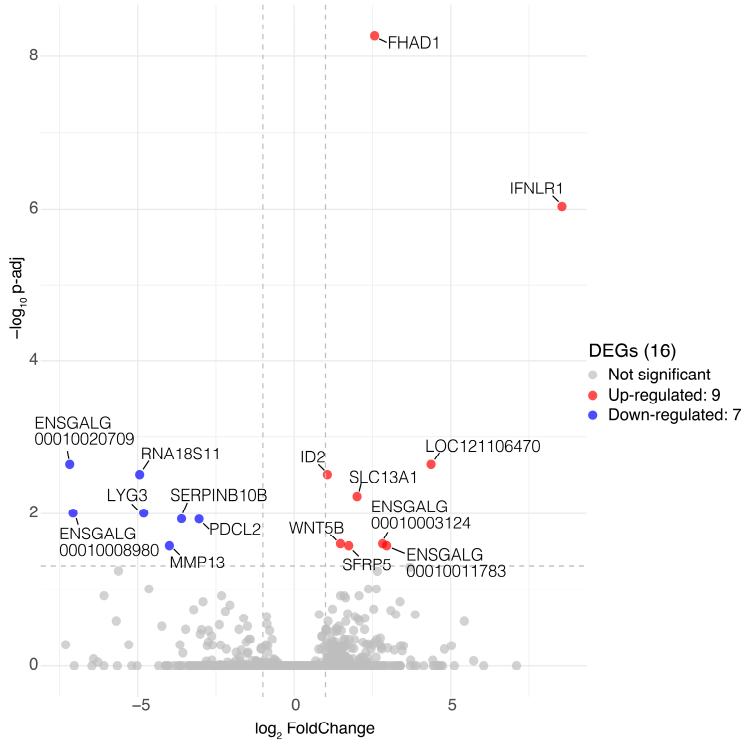


Figure 6. Volcano plot (scatterplot) for genes in ovarian tissues that differ in expression level between the two groups of laying hens, PP and DP. The distribution of all genes is shown at the threshold p-adj < 0.05. The x-axis represents the $\log_2$ fold change ($\log_2$FC), i.e., the logarithm of the ratio of gene expression in the PP group compared to the DP group. The y-axis represents the $-\log_{10}$ values for p-adj that reflect the significance of differences in gene expression, converting low p-values into large positive numbers to facilitate visualization. Each point on the graph represents one gene. Genes with a p-value less than the threshold and an absolute $\log_2$FC value greater than the threshold are considered significant DEGs and are highlighted in red and blue. Genes with no significant expression changes are shown in gray. On the right side, the dots conform to upregulated genes in the PP group, and the dots on the left side to upregulated genes in the DP group. The horizontal dashed line represents the threshold for statistical significance ($p < 0.05$), while the vertical lines represent the threshold for the magnitude of expression change ($|\log_2\text{FC}| \geq 1$).

Of particular interest is the modulation of the signaling pathway gene *WNT5B* (Table 3). In the PP group of chickens, a higher *WNT5B* upregulation was observed (175.52 vs. 62.61 in DP; $\log_2$FC = 1.48, p-adj = 0.025). Also, a greater *SFRP5* expression was established in the PP group (243.65 vs. 73.31 in DP; $\log_2$FC = 1.74, p-adj = 0.027). On the other hand, the DP group was characterized by activation of the *MMP13* gene expression 16 times higher than in PP ($\log_2$FC = −3.99, p-adj = 0.027). The expression level of the *ID2* (inhibitor of DNA binding 2, HLH protein) gene in the PP group was significantly higher than that in the DP group ($\log_2$FC = 1.06, p-adj = 0.003; Table 3).

3.6. Evaluation of the Hierarchical Topology of Significant Genetic Determinants

Analysis of normalized expression levels using nonlinear hierarchical approximation revealed the presence of pronounced structural differences in the transcriptome pattern between the PP and DP chicken groups. A similarity in the amplitude of the network ordering signal K was noted in both groups (PP and DP; ~1.50×10^{-4}; Table 4). However, a critical difference in the reliability of the model was observed (R^2 = 0.95 vs. 0.62 for PP and DP, respectively). In addition, a significant basal expression level was revealed in the PP group (α = 36.25, $p < 0.01$). In contrast, the DP group exhibited a value of α = 45.05 (p = 0.276).

Table 4. Parameters (M ± SEM) [1] of the additive exponential model based on the top 16 DEGs in ovarian tissues of laying hens from the PP and DP groups.

Parameter	Symbol	PP Group (n = 3)	DP Group (n = 3)	Difference (Δ, %)
Baseline expression level (noise)	α, arbitrary units	36.25 ± 12.24	45.05 ± 40.86	24.3
Significance level of parameter α	p-value	0.005	0.276	–
Amplitude of the regulatory response	K, arbitrary units	$1.498 \times 10^{-4} \pm 5.100 \times 10^{-6}$	$1.485 \times 10^{-4} \pm 1.700 \times 10^{-6}$	−0.9
Significance level for K	p-value	<0.001	<0.001	–
Determination coefficient	R^2	0.949	0.621	−34.6

[1] M, mean; SEM, standard error of the mean.

3.7. Validation of Candidate Gene Expression Profiles via RT-qPCR

The transcription dynamics of seven selected target genes were evaluated via RT-qPCR to confirm the expression trends observed in the high-throughput transcriptomic pipeline. The comparative analysis demonstrated close directional alignment between the RNA-Seq $\log_2$FC metrics and the qPCR relative quantification values. The corresponding fold-change data, reflecting the transcriptional shifts between the PP and DP cohorts, are summarized in Table 5.

Table 5. Relative expression folds of predictive candidate genes linked to reproductive longevity in the PP and DP hen cohorts validated via RT-qPCR (n = 3).

Group	*ID2*	*SFRP5*	*SERPINB10B*	*LYG3*	*AvBD4*	*HSPB9*	*MMP13*
PP group	1.00	1.00	1.00	1.00	1.00	1.00	1.00
DP group	0.07 ***	0.03 ***	16.00 ***	3.86 *	1.02	1.18	9.02 **

Note: Data are expressed as relative fold changes against the PP baseline (set as 1.00). Statistical significance was determined using Student's t-test: * $p < 0.05$, ** $p < 0.01$, *** $p < 0.001$, indicating significant differences in the DP group compared to the PP group.

The RT-qPCR validation confirmed that, while the absolute fold-change values in some instances quantitatively differed from the deep sequencing dataset, the overall expression trends (i.e., the direction of upregulation or downregulation) were highly consistent for five out of the seven analyzed loci. Specifically, two genes (*ID2* and *SFRP5*) exhibited a profound and highly significant downregulation in the DP group compared to the PP baseline ($p < 0.001$), aligning with the RNA-Seq results where these loci were significantly enriched in PP hens.

Conversely, the transcription levels of *SERPINB10B*, *MMP13*, and *LYG3* were significantly upregulated in DP birds by 3.86- to 16.00-fold ($p < 0.05$), corroborating the transcriptomic sequencing trends. In contrast, the expression profile of *HSPB9* and *AvBD4* showed no statistically significant differences between the two phenotypic groups.

4. Discussion

The wild ancestor of modern chickens, the red junglefowl (*G. gallus*), has a naturally lower reproductive ability compared to its domesticated counterparts [77,97]. The reproductive system of chickens is a complex self-regulating system in which the processes of folliculogenesis, steroidogenesis, angiogenesis and apoptosis are in dynamic equilibrium [98]. Changes in the expression of genes associated with the activation of matrix metalloproteinases (MMPs) [99], induction of apoptotic signaling pathways or disruption of immune

homeostasis in ovarian tissue can, however, trigger early follicle involution [100]. This, most likely, results in a decrease in egg-laying intensity. Recent advances in high-throughput sequencing (RNA-Seq) offer a unique opportunity to study this complex system and identify molecular profiles of productivity and reproductive longevity [20]. Various chicken breeds and crosses have genetically determined differences in ovarian gene expression and signaling pathways regulating the egg-laying cycle [101–103]. Transcriptomic profiling in reproductive organs and cells allows the identification of key genes involved in follicle development, ovulation, and other fundamental reproduction-related processes [104]. To date, however, the molecular mechanisms that determine the transition from stable ovarian function to the premature regression phase remain poorly understood [20]. In this study, we identified some key genetic determinants underlying the long-term physiological resource of egg production at the level of ovarian function.

4.1. Morphometric Adaptations and Systemic Physiological Status

The observed macromorphological alterations in internal organs underscore a profound divergence in physiological resource allocation between the high- and low-performing hen phenotypes. The significant increase in liver weight documented in the late-degraded production (DP) group implies a shift in vitellogenesis dynamics. In avian physiology, the liver serves as the exclusive site for vitellogenin and very-low-density lipoprotein (VLDL) synthesis, which are critical precursors for egg yolk formation [105]. An enlarged hepatic mass, when paired with the concurrent 11.4% increase in abdominal fat deposition observed in DP hens, strongly points toward localized lipid accumulation (hepatic steatosis) and inefficient precursor transport rather than enhanced reproductive synthesis. This hepatic strain is further corroborated by the 1.3-fold upregulation of ALP activity in the DP group, a classic serum biomarker indicative of cholestasis or compromised hepatocyte membrane integrity in poultry [106].

This metabolic strain appears tightly intertwined with a dampening of the neuroendocrine reproductive axis. In contrast to the liver and abdominal fat, both comb weight and comb length were significantly reduced in the DP group. Because the avian comb is a highly hormone-dependent secondary sexual characteristic whose development is directly regulated by circulating estrogens (primarily β-estradiol) [107], this striking phenotypic regression signals a systemic hypoestrogenic state in DP hens, likely contributing to their delayed plateau onset and rapid decline in laying persistence.

Although all hematological and biochemical profiles remained within acceptable physiological boundaries [96], fine-grained variations between the cohorts reveal distinct systemic adaptations. The DP hens exhibited moderate yet statistically significant reductions in RBC count, hemoglobin concentration, and blood color index. This cluster of traits typically reflects a lower hemoglobin saturation capacity per erythrocyte and may stem from altered iron utilization or minor deficiencies in hematopoietic cofactors, such as vitamin B_{12} and folic acid [108]. Crucially, the combination of lower circulating hemoglobin alongside an increased PCV in DP hens serves as a hallmark of hemoconcentration and altered fluid balance. In poultry, this specific hematological configuration is frequently associated with metabolic syndrome, visceral adiposity, and elevated body condition scores [109]. The observed decrease in serum total protein and β-globulin fractions (which comprise key transport proteins like transferrin and specific lipoproteins) further substantiates a systemic disruption in nutrient and iron trafficking within the DP cohort [110]. Concurrently, the elevations in SBA and IgG levels in the DP cohort point toward an augmented humoral immune response [111]. This systemic shift aligns closely with our ovarian transcriptome data, which revealed an upregulation of immune-response-associated loci (e.g., *AvBD4* and *SERPINB10B*) in late-degraded hens. Furthermore, the

1.3-fold increase in ALP activity observed in DP birds implies notable alterations in lipid metabolism and hepatic function [112], mirroring the differential expression signatures of lipid transport genes identified within the ovarian microenvironment.

Perhaps the most intriguing finding is the apparent metabolic trade-off between chronic immune activation and reproductive performance. The DP cohort exhibited a 28.7% enlargement in splenic mass alongside elevated SBA and increased IgG levels. While a robust humoral response and splenic hypertrophy are traditional markers of complement system activation and immune readiness [113], their upregulation in low-producing birds highlights a compelling evolutionary and physiological compromise. Maintaining a hyper-reactive immune status is energetically expensive. These findings suggest an immune-mediated resource reallocation strategy: the DP hens appear to "squander" vital metabolic and amino acid resources on sustaining a low-grade, persistent immune or inflammatory response, thereby starving the hypothalamic–pituitary–ovarian axis of the energy vectors required to maintain an extended egg-laying plateau [114].

4.2. Quality of Transcriptome Data

The generated transcriptome data from ovarian tissues of Dekalb White laying hens with contrasting egg production phenotypes—early and stable vs. late and degraded—demonstrated sufficient technical reliability of the method and high quality of the data (Table 2). Taken together, a detailed transcriptomic profile formed by a significant number of high-quality reads was characterized for all analyzed samples, which was in line with similar studies (e.g., [115]). Our data provided the required sequencing depth. Key sequencing quality metrics indicated the high accuracy of the obtained primary data, which is a critical condition for reducing the likelihood of errors in subsequent stages of analysis [116].

Conforming to the best practices for RNA-Seq data analysis [116] the performed procedure for mapping reads to the *G. gallus* GRCg7b reference genome was also consistent with the high quality of the prepared transcriptome libraries. The high percentage of successfully mapped reads pointed out the specificity of the obtained data and the absence of significant contamination [116]. Furthermore, the observed percentage of reads mapping to multiple genomic positions was within the acceptable limits [117].

The transcriptome libraries' guanine and cytosine contents (45–46%; Table 2) matched the anticipated nucleotide composition for the species *G. gallus* [118].

4.3. Transcriptome Profile Depending on the Productive Plateau Dynamics

The PCA-assisted exploration of transcriptome profiles (based on the 500 most variable genes) revealed a clear division of all samples into two clusters that conformed to the PP and DP groups of chickens (Figure 1). PC1, which explained 64.9% of the total data variance, was the main factor determining this division [119] and indicated significant differences in gene expression regulation patterns between the groups. PC2, describing 14.3% of the variation, is known to reflect mainly the variation between biological replicates within each group in the RNA-Seq analysis [120]. In our opinion, and according to the DGE analysis methodology [121], the high degree of clustering of biological replicates within the corresponding groups was a sufficiently significant prerequisite for the subsequent reliable identification of DEGs.

The PCA-based transcriptome differences detected at the overall level (Figure 1) were specifically confirmed by our results of DGE analysis. Profound transcriptome rearrangements revealed the nature of regulation in the studied bird groups (Figures 2, 3 and 6). In the PP phenotype, the response was localized and concentrated in a major fraction of the most significant DEGs (Figures 3 and 6). In contrast, the response in DP birds took on the character of a global shift expressed in the activation of alternative pathways at the

level of the overall ovarian transcriptome, as confirmed by the negative enrichment index (NES) (Figure 2). This specificity of the response indicates transcriptional inversion and a functional switch in the genetic system in the studied bird groups. The wide range of changes in mRNA levels between groups, encompassing 484 genes (Figures 2 and 3), likely indicates a significant reorganization of the ovarian tissue transcriptome depending on the nature of the productive plateau. Interestingly, the majority of these changes (305 genes) were enhanced in the PP group, which may suggest the activation of specific molecular mechanisms that support long-term high egg production [122].

4.4. Functional Interpretation of the Identified Expression Patterns

Further functional analysis of the identified DEGs using the KEGG and GO databases allowed us to detail the predicted biological processes that may be associated with phenotypic differences between the studied hens' groups. The spectrum of functional categories found here, including enzymatic activity (in particular, lipase), carbohydrate metabolism, metabolite transport and immune response, allows us to suppose a probable range of molecular processes associated with the different dynamics of the productive plateau (Figure 4). The significant changes detected in the transcriptional profile of the PP hens' ovaries may be related to the formation of deep metabolic tissue specialization necessary for maintaining high reproductive function over a long period [123].

The GSEA approach we applied to a set of highly significant genes allowed us to identify key regulatory nodes, while minimizing the influence of background transcriptomic noise. This is consistent with the current methodology for analyzing predicted metabolic profiles [83]. Induction of the *PNLIPRP1* gene expression demonstrates the importance of lipase activation in shaping the functional profile of the PP layers (Figure 4). Such a shift supports the hypothesis that lipid breakdown and lipid depot remodeling processes predominate in the ovaries of high-yielding birds, providing the energy requirements for intensive folliculogenesis. Activation of lipase activity associated with the highly expressed *PNLIPRP1* gene in the PP group can apparently be considered as a regulatory mechanism that ensures the mobilization of lipid resources to maintain a long-term productive plateau [124]. These results confirm previously stated assumptions about the dominant role of lipid catabolism and lipid depot remodeling in the ovaries of highly productive birds [83,125]. Opposite dynamics of expression of the genes involved in lipase activity (*PNLIPRP1*) and phospholipid transfer (*PLTP*), observed in other studies [125] and herein in the PP group, is consistent with the concept of redistribution of energy substrates in chickens exhibiting high productivity [126]. Such multidirectional dynamics may indicate a switch of metabolism in the group with high productivity stability to the preferential use of internal intracellular lipid resources of the ovary [127]. Using the complete transcriptome dataset, the prevalence of processes associated with the activity of chemokine and cytokine receptors, as well as lipopolysaccharide binding, was revealed (Supplementary Figure S1). Such a global orientation towards the receptor systems of innate immunity is consistent with the concept of systemic redistribution of resources in highly productive poultry crosses [83]. Similarly, pronounced activation of the *CPLX1* expression, which plays a key role in regulating transmembrane transport and the neuroregulatory function [128], was detected in the ovarian tissues of PP chickens. This likely manifests as an intensification of follicle maturation processes and high secretory activity, both of which are necessary for maintaining reproductive function [129].

Preliminary trends observed within the DP cohort point toward potential systemic immune dysregulation, a finding that aligns with prior observations [130]. In particular, the *AvBD4* gene, a key antimicrobial peptide [131–133], was significantly upregulated in the ovary of DP chickens. In clinically healthy birds, such overexpression may indicate an

increased immune tone in the reproductive tissue [134], which can negatively affect folliculogenesis [135]. Significant energy expenditure on the synthesis of immune factors can create a metabolic load that competes with the resources required by granulosa cells [136].

The pattern of molecular adaptations in the PP group was complemented by a pronounced induction of the expression of the *HSPB9* gene that encodes an ATP-independent molecular chaperone belonging to the small heat shock protein family. Upregulation of *HSPB9* was probably indicative of more effective protection of proteins from denaturation under conditions of oxidative stress accompanying intense stress on the reproductive system [137]. While other researchers observed an increase in *HSP70* and a specific polymorphism in this gene in low-producing hens [138], the induction of *HSPB9* in high-producing layers may suggest a specific adaptive mechanism for protecting ovarian tissue.

4.5. Network Analysis and Identification of Key Regulatory Nodes

It is well established [121] that DGE analysis in combination with network analysis allows for the identification of key genetic determinants based on their individual significance and network centrality. Our network analysis using the MCC algorithm revealed a group of highly connected hub genes (*TLR4*, *TLR7*, *TLR2A*, *LY86*, and *TLR1A*), apparently associated with the immune status of the ovaries of laying hens [139]. The high functional involvement score and significant number of connections of these nodes likely indicate that these genes may be important control points. These hub genes are central to maintaining the network stability and structure, and their dysregulation may result in compounded genetic effects [140]. In addition, network analysis revealed a cluster including the *SFRP5*, *WNT5B* and *MMP13* genes (Figure 5). Despite a relatively small number of internal connections, this block is functionally integrated into the overall transcriptome network through the central *ALB* node, which may indicate its potential role in the regulation of ovarian function [141]. The identified *SFRP5–WNT5B–MMP13* regulatory cluster may represent a functional node reflecting a key aspect of the physiological state of ovarian tissue [127,142].

4.6. Benjamini–Hochberg Correction Results: 16 Key Candidate Genes

To minimize false-positive results that are inevitable when performing multiple comparisons of thousands of transcripts [143], a stringent statistical test with correction for multiple testing using the Benjamini–Hochberg method [79,144] was applied. This approach is believed [143] to control, with a high degree of probability, a significant proportion of false discoveries among the many genes declared as DEGs. Without such correction, the number of false-positive results can become unacceptably high when testing multiple hypotheses [145]. This approach allows one to identify with a high degree of confidence key candidate genes whose expression changes are least likely to be an artifact of multiple testing [143].

Our analysis revealed 16 highly significant DEGs (Figure 6, Table 3). Some lacked detailed functional annotation in available databases (Ensembl, NCBI), which currently complicates their interpretation in the context of ovarian function. Their high statistical significance, however, makes them promising targets for subsequent functional studies.

A significant proportion of genes with known functional annotation (*SLC13A1*, *ID2*, *MMP13*, *SERPINB10B*, *PDCL2*, *WNT5B*, *LYG3*, *IFNLR1*, *SFRP5*, *FHAD1*, *LOC121106470*) may be directly or indirectly involved in the regulation of key processes maintaining ovarian homeostasis, such as cell cycle and apoptosis control, immunity, morphogenetic signaling pathways, extracellular matrix (ECM) remodeling and cellular stress response [146,147]. Importantly, *SERPINB10B* is a member of ovalbumin-related serpins (ov-serpins) in birds [148] that belong to a broader serpin superfamily with cytoprotective functions [149]. A cluster of ov-serpins, including, among others, *SERPINB10B*, *SERPINB14* (ovalbumin, or *OVAL*),

SERPINB14B (ovalbumin-related Y, or *OVAY*) and *SERPINB14C* (ovalbumin-related X, or *OVAX*) in the chicken is located on a 150 kb locus chromosome 2q [148]. This suggests that *SERPINB10B* may be involved in reproduction and egg formation, although its exact role needs an in-depth investigation.

The finding that the genes forming the structurally identified network cluster (*SFRP5*, *WNT5B* and *MMP13*; Figure 5) are also the statistically most significant DEGs is an interesting observation (Table 3, Figure 6). Indeed, the Wnt signaling pathway is a highly conserved regulator of key cellular processes, including proliferation, migration, survival, and cell fate determination [146]. In PP chickens, *WNT5B* upregulation can ensure the correct spatial orientation and adhesion of granulosa and theca cells, which is a prerequisite for the formation and maintenance of a healthy follicle hierarchy [150]. The importance of this pathway for ovarian function and productivity in chickens is also supported by previous studies. In particular, a comparative analysis of the ovaries in Jinghai Yellow chickens with high and low egg production identified the Wnt signaling pathway as one of the key differentially regulated pathways [151,152]. Notably, this study [152] showed the *WNT4* (Wnt family member 4) gene as a highly expressed candidate directly associated with the regulation of egg production, which is also supported by a study of polymorphisms in this gene [152]. These data, together with our results on upregulation of the *WNT5B* ligand gene in the PP group, may suggest that enhanced activation of Wnt signaling in the ovaries is a specific feature associated with maintaining high reproductive efficiency [153]. Sun et al. [154] also demonstrated in their transcriptome analysis of laying hen ovarian tissue that a number of signaling pathways, including the interaction of neuroactive ligands with receptors, play a critical role in follicle selection and increased egg production. These authors identified candidate genes, such as *NDUFAB1* (NADH:ubiquinone oxidoreductase subunit AB1) and *GABRA1* (gamma-aminobutyric acid type A receptor alpha1 subunit), that regulate ovarian development in opposite directions. *NDUFAB1*, on the other hand, stimulates granulosa cell proliferation, suppresses apoptosis and enhances steroidogenesis (through the expression of *STAR* (steroidogenic acute regulatory protein) and *CYP11A1* (cytochrome P450 family 11 subfamily A member 1)). *GABRA1*, conversely, inhibits these processes.

In contrast, *SFRP5* upregulation in the PP group of chickens may imply a link between lipid metabolism and effective ovarian function [147,155]. Also, according to the studies by Maman et al. [147], SFRP5 protein induction is part of the normal process of follicle maturation in humans. It is likely that healthy, highly functional granulosa tissue in PP chickens is capable of adequately responding to hormonal signals, including *SFRP5* expression for precise control of morphogenic processes during follicular growth and ovulation.

In this regard, the pronounced upregulation of the *MMP13* gene in the DP group of egg-laying hens (an almost 16-fold increase we detected during our analysis) is of particular interest. In our opinion, this result is consistent with the known role of MMPs in ECM remodeling during physiological and pathological processes [156]. An investigation by Yuan et al. [157] showed that the expression of this gene in the ovaries of hens increases consistently with maturation, reaching a peak by Day 159, which may be associated with the processes of intensive ECM remodeling during atresia and regression. It has previously been suggested that fine-tuning of *MMP9* (matrix metallopeptidase 9) expression in chicken ovaries may promote efficient follicle maturation and ovulation, and that polymorphisms in the *MMP9* gene promoter are associated with egg production traits [157,158]. In chickens, the MMP13 protein is localized in stromal cells, thecal layers of follicles of all sizes, and primordial follicles [157]. Notably, polymorphisms in the promoter region of the *MMP13* gene are associated with such an important selection trait as the age at onset of egg laying [157]. Thus, *MMP13* upregulation observed in our study may signal a possible dysregulation of a key proteolytic system that controls the balance between physiological renewal and

pathological destruction of follicular tissue [157]. Based on this, it can be speculated that a more balanced expression of the *SFRP5–WNT5B–MMP13* cluster components appears to be associated with the maintenance of prolonged productivity, whereas an imbalanced *MMP13* overexpression likely reflects a condition characterized by matrix dysregulation and potential loss of follicular reserve [157].

The identified *SFRP5–WNT5B–MMP13* triad highlights a stark expression contrast between the PP and DP cohorts, underscoring a pivotal role of the Wnt signaling pathway in managing these phenotypes. These genes are critically involved in regulating ECM remodeling and maintaining follicular tissue homeostasis. The synchronous upregulation of *WNT5B* and *SFRP5* observed in the PP group suggests a finely tuned activation of non-canonical Wnt signaling coordinated to preserve the structural and functional integrity of the ovarian ECM. Conversely, the DP group is characterized by a pronounced overexpression of *MMP13*, which points toward a disruption in Wnt-mediated tissue maintenance, leading to accelerated follicular proteolytic degradation and impaired tissue nourishment [156,157]. Such a pronounced shift toward destructive, catabolic processes may ultimately trigger premature follicular reserve depletion, explaining the rapid degradation of the egg-laying plateau.

Upregulation of the *ID2* gene expression in PP chickens (Table 3), in all likelihood, can be considered as a modulation of key transcriptional events occurring within granulosa cells during or immediately after differentiation at different stages of follicle development [159]. The *ID2* gene is known as one of the significant molecular mediators of signaling molecules playing an important role in embryogenesis and development, as well as in maintaining tissue homeostasis in adults [160]. It has been shown that proteins of the ID (inhibitor of DNA binding) family are dominant-negative regulators of helix–loop–helix transcription [161]. They form heterodimers with bHLH (basic helix–loop–helix) proteins, thereby participating in the regulation of cell proliferation/differentiation [162]. In a sheep ovary model, it was shown that *ID* genes are constantly expressed in steroidogenic cells throughout follicle development, while their decrease in thecal cells is a sign of atresia [159]. Thus, high *ID2* expression in the PP group may indicate a specific mechanism for maintaining follicle viability. This is also supported by transcriptome analysis of chicken granulosa cells, where the *ID2* gene was identified as a critical factor involved in intensive cell division [163].

4.7. Structural Topology and System Stability

Standard DGE analysis, as well as network analysis, are generally unable to provide a comprehensive understanding of the systemic integration and hierarchical stability of the identified assemblies [164]. To overcome this limitation, we implemented an integrated approach that complements topological analysis with mathematical approximation methods based on the principles of fractal geometry [91,165]. This approach allowed us to characterize quantitatively the systemic organization of the network for genes that passed the statistical significance threshold [166]. Within the framework of this methodology, high values of the coefficient *K* were interpreted as an indicator of the hierarchical ordering of the network (i.e., network integration), while a decrease in the approximation accuracy (R^2) indicated the degradation of the holistic structure and an increase in entropic noise [167].

The results of our analysis suggest the presence of pronounced structural differences in the ovarian transcriptome organization between the chicken groups as also shown in other studies (e.g., [168]). The similarity in the amplitude of the network ordering signal *K* in both groups implies the presence of comparable regulatory potential (Table 4) [169]. However, the critical difference in the model reliability (R^2 = 0.95 vs. 0.62 for PP and DP, respectively) probably shows that this potential in the PP group is likely realized

through a rigid hierarchical structure, whereas it manifests itself in the mode of systemic destabilization in the DP group [167,169].

In the context of informational complexity, the baseline expression level α reflects the magnitude of background stochastic noise within the transcriptional network [166]. Accordingly, the PP group, with a significantly lower and well-defined α value ($p < 0.01$), was likely characterized by a higher potential for maintaining long-term reproductive productivity. The stability of this parameter in PP chickens may indicate a reliable and highly canalized transcriptional baseline, ensuring a robust functional tissue reserve. Conversely, the DP group exhibited a pronounced degradation in the predictability of the baseline gene expression level α ($p = 0.276$, $R^2 = 0.62$). Biologically, this loss of statistical significance and model fit can be interpreted as an inflation of network entropy and the erosion of the baseline regulatory plateau. This transcriptional destabilization implies that the DP phenotype operates in a stochastic noise mode, where loose network integration replaces coordinated control. Thus, a stable, highly predictable hierarchy of regulatory interactions is a fundamental prerequisite for sustaining high productivity potential [91,170].

Collectively, the use of a specialized mathematical model [91], in addition to standard DEG analysis, has enabled us to move beyond the description of individual genes to a quantitative assessment of the systemic organization of the follicular transcriptome and its dynamic changes [171]. According to our data, as well as previously known principles of network biology, the regulatory networks of highly productive animals should exhibit pronounced scale-free properties and self-similarity, ensuring their functional stability [172].

4.8. Integration and Methodological Validation of Transcriptomic Signatures via RT-qPCR

The strategic selection of candidate genes for RT-qPCR verification was guided by two primary criteria: the magnitude of differential expression and the overarching biological significance of the respective loci [124,130]. This robust multi-pronged approach enabled the construction of a customized validation panel comprising seven key genes that reflect diverse functional dimensions of the divergent poultry phenotypes.

The real-time amplification profiles demonstrated a high directional concordance, with eight out of the five out of the seven analyzed loci (~71.4%) displaying identical regulation trends (i.e., upregulation or downregulation) in the DP group relative to the PP baseline. This significant concordance substantiates the technical reliability and accuracy of our high-throughput RNA-Seq data-processing pipeline. It is worth noting that while the absolute fold-change values in some instances quantitatively differed between the two methodologies, the fundamental transcription trajectories remained strictly preserved. Such numerical variances are deeply rooted in the distinct mathematical normalization algorithms, detection chemistries, and technical sensitivities inherent to RNA-Seq and RT-qPCR platforms [173].

Mechanistically, the striking 16.00-fold transcriptional acceleration of *SERPINB10B* coupled with the 9.02-fold upregulation of *MMP13* in the DP group (Table 5) provides compelling evidence of localized tissue-remodeling stress. MMP13 is a potent collagenase inherently linked to structural ECM degradation. Its heightened expression in late-degraded hens strongly suggests an accelerated breakdown of the ovarian follicular framework, which likely impairs healthy folliculogenesis and drives the rapid post-plateau degressive productivity phase. Conversely, the profound silencing of *ID2* (0.07-fold) and *SFRP5* (0.03-fold) in DP birds (confirming their robust upregulation in the PP cohort) underpins the molecular basis of egg-laying plateau persistence. ID2 plays a fundamental role in maintaining cellular differentiation and suppressing premature senescence within follicular granulosa cells. Concurrently, the upregulation of *SFRP5* (a canonical Wnt pathway antag-

onist) in PP hens acts as a crucial homeostatic buffer, modulating excessive Wnt-mediated signaling that could otherwise trigger apoptotic cascades and tissue inflammation.

A notable discrepancy was observed regarding the *HSPB9* and *AvBD4* loci. While the initial RNA-Seq analysis suggested a rapid and sharp elevation of *HSPB9* and *AvBD4* expression in the PP cohort, this pattern was not experimentally corroborated by the subsequent RT-qPCR validation, which revealed no statistically significant differences between the groups. This lack of confirmation does not necessarily label the deep-sequencing discovery as a false positive. Euthanasia via cervical dislocation represents an ethically approved, standard protocol for experimental poultry studies; however, the associated physical trauma and absence of pre-sedation can induce an acute, ultra-fast physiological stress response. This immediate cascade is known to trigger the rapid transcription of heat shock proteins (HSPs), transcriptomic factors, and molecular chaperones [174]. Given that the majority of our key candidate genes (such as *ID2*, *SFRP5*, and others) demonstrated impeccable directional concordance between the two methods, the variation in *HSPB9* and *AvBD4* is likely a technical manifestation of differential sensitivity to immediate post-mortem stress responses.

Ultimately, the high level of directional consistency achieved through these two independent methodological frameworks serves as a powerful testament to the baseline validity of the uncovered genetic markers. Nevertheless, to further establish their definitive functional roles, validate downstream tissue-specific translations, and evaluate their practical applicability in marker-assisted breeding programs, future large-scale validation studies utilizing expanded validation cohorts and direct functional assays would represent the logical next step of investigations.

4.9. Study Limitations

One of the primary limitations of the present work is the utilization of an extreme-phenotype sampling design. Out of an initial pool of 60 birds per cohort, only three individuals exhibiting the most contrasting zootechnical and phenotypic traits were selected for RNA sequencing. While this strategy was explicitly employed to minimize random individual biological noise and has been successfully implemented in previous avian whole-transcriptome studies [43,56], the small sample size (n = 3 per group) partially constrains the broader statistical generalization of the dataset. Crucially, rather than employing a random distribution within the cohorts, these three biological replicates were chosen through a stringent, non-random rule based on a comprehensive matrix of zootechnical indicators (Supplementary Table S2). Birds representing the absolute extreme polar ends of the phenotypic distribution for each group were intentionally isolated. This targeted extreme-phenotype design was strategically deployed to suppress confounding intra-group biological variability artificially. In small-scale omics studies, random sampling frequently risks capturing irrelevant individual baseline noise, which reduces statistical power. By selecting individuals with highly pronounced, unmistakable phenotypic deviations, we maximized the probability of identifying true, biologically significant DGE signatures inherently tied to the reproductive plateau itself. Nonetheless, while this deliberate selection strategy maximized the contrast within our low-volume screening, the small sample size dictates that these identified molecular markers and transcriptional signatures should be treated as strictly exploratory. Consequently, their definitive verification will necessitate further validation in larger, more representative poultry cohorts.

Regarding sample processing, certain methodological boundaries must be acknowledged when interpreting the transcriptomic data. To guarantee the highest possible RNA integrity and prevent enzymatic or chemical degradation, histological staining protocols (e.g., hematoxylin and eosin) were intentionally omitted from the immediate sampling

pipeline. The application of chemical fixatives and aqueous dye solutions is widely recognized to cause significant fragmentation of total RNA, which would severely compromise the accuracy of high-throughput sequencing [175]. Instead, the morphological homogeneity of the ovarian replicates was evaluated using stereomicroscopic visualization under a binocular microscope. While this approach effectively standardized the samples across macro-structural parameters (ensuring consistent tissue color, density, and the absolute exclusion of macro-vessels or follicles exceeding 1 mm), it cannot completely rule out microscopic cellular heterogeneity or minor variances in early follicular development stages. Because bulk RNA sequencing captures a pooled cellular transcriptomic signature, the discrete molecular contributions of individual follicles at slightly varying micro-developmental stages cannot be entirely isolated. Nevertheless, because all selected tissues strictly contained follicles under 1 mm and underwent identical stereomicroscopic screening, any internal variation is considered minimal and systematically uniform across all biological replicates. While individual biological variability between birds inherently influences gene expression profiles, this variance was mathematically factored into our rigorous differential expression pipeline using DESeq2 normalization models.

Turning to the experimental validation phase, the cohort size utilized for RT-qPCR verification may limit the overall statistical power of the validation assay. At this stage of the investigation, the verification panel was strategically restricted to seven candidate genes prioritized from the broader pool of differentially expressed loci; as a result, these verification trends cannot be directly extrapolated across the entire transcriptomic landscape. It must also be emphasized that functional validation assays and direct assessments of downstream protein expression levels were not performed in this study. While these transcriptomic signatures provide high-resolution insights into mRNA accumulation patterns, further proteomic and functional analyses are required to conclusively establish the definitive biological translation of these molecular markers.

Finally, a parallel limitation applies to the hematological, biochemical, and morphometric evaluations of internal organs. While this replicate number is sufficient for high-throughput sequencing exploration, it remains statistically constrained for drawing generalized conclusions regarding systemic physiological or immunopathological states. Hence, all hematological, biochemical, and necropsy data should be strictly interpreted as preliminary trends that require validation in expanded cohorts with larger animal populations. We refrain from making definitive claims regarding systemic dysregulation or metabolic disorders based on these parameters alone; rather, these data should be viewed as exploratory findings providing a conceptual baseline for future large-scale confirmatory research.

5. Concluding Remarks and Further Prospects

In this study, we explored the transcriptomic profiling of ovarian tissue (stroma with cortical follicles) from Dekalb White laying hens with contrasting egg production phenotypes, specifically early-persistent (PP) vs. late-degraded (DP) production cohorts. A total of 484 DEGs were identified, the characterization of which suggests potential molecular determinants that may be associated with the maintenance of high ovarian persistence. The range of identified functional categories (encompassing lipase activity, carbohydrate metabolism, metabolite transport, and humoral immunity) points towards a complex network of candidate molecular processes associated with the varying dynamics of the productive plateau. In the PP cohort, the observed structural induction of the *PNLIPRP1* gene suggests a focus on lipid breakdown and redistribution processes in the ovaries, which could theoretically support the substantial energy requirements of intensive folliculogenesis. The contrasting dynamics of expression between the lipase-associated (*PNLIPRP1*) and the phospholipid transfer (*PLTP*) genes in the PP group are consistent

with the hypothesis of a targeted redirection of energy substrates to maintain a prolonged productive plateau.

Applying a stringent statistical test with correction for multiple testing to minimize false-positive results, we demonstrated that the PP egg-laying phenotype appears to be characterized by the coordinated activation of 16 genes. Among the functionally annotated loci, the most pronounced transcriptional shifts were observed for *SLC13A1*, *ID2*, *MMP13*, *SERPINB10B*, *PDCL2*, *WNT5B*, *LYG3*, *IFNLR1*, *SFRP5*, *FHAD1*, and *LOC121106470*. In particular, the coordinated induction of the Wnt signaling pathway components (*WNT5B* and its antagonist *SFRP5*), alongside the upregulation of the *ID2* gene, represents a candidate intraovarian environment potentially associated with the preservation of the follicular reserve and the suppression of premature atresia. Conversely, the marked 9.02-fold upregulation of the *MMP13* collagenase gene in the DP cohort points to a possible intensification of ECM destruction processes that may accompany the onset of the degressive egg-laying phase.

Mathematical modeling revealed that the transcriptomic profile of PP egg laying is characterized by higher systemic robustness, reinforced by an organized hierarchy of regulatory interactions, which is hypothesized to support the resilience of regulatory networks to external and internal negative impacts. At the same time, destabilization of background expression and decreased systemic resilience may represent potential prerequisites for early termination of the egg production cycle. The identified genes represent a promising candidate panel for the exploratory study of individual reproductive longevity, offering conceptual opportunities for the future development of molecular breeding strategies in laying hens to maintain high egg production without the use of forced-molting techniques. Overall, while constrained by the sample size, these pilot data provide a suggestive theoretical basis for developing approaches to support the functional state of the reproductive system in poultry.

To validate these high-throughput sequencing data, a custom panel of seven candidate genes was strategically selected based on their expression magnitude and functional relevance to avian reproductive biology. Quantitative real-time PCR (RT-qPCR) validation demonstrated strong directional concordance with the whole-transcriptomic profiles, with the five out of the seven analyzed loci (~71.4%) exhibiting identical regulation trends in the DP group relative to the PP baseline. Although the absolute fold-change values quantitatively varied between the two methodologies in certain instances (a phenomenon inherently tied to platform-specific normalization algorithms and sensitivities), the overarching transcriptional trajectories remained strictly preserved. This high level of directional consistency across two independent methodological frameworks reinforces the technical reliability of the uncovered genetic markers and underscores their potential prognostic value for assessing reproductive persistence in hens.

Additionally, the morphometric and hematological variations observed between the cohorts (such as differences in liver and spleen mass, comb development, erythrocyte profiles, and SBA levels) suggest that alterations in egg-laying performance may be accompanied by subtle systemic metabolic and immunological shifts that extend beyond the transcriptomic framework. However, it is essential to emphasize that these discrepancies are not entirely definitive and represent suggestive physiological trends rather than sustained pathological changes. Consequently, establishing more robust conclusions regarding the significance of these systemic realignments will require subsequent investigations utilizing larger sample sizes alongside a broader array of biochemical and functional assays.

To expand upon these exploratory trends, our subsequent research phase will focus on profiling circulating hormones, including estradiol, progesterone, corticosterone, and thyroid hormones. This endocrinological characterization will help elucidate reproductive regulation at the systemic level and facilitate direct correlations with the identified gene

expression signatures. Additional histopathological evaluation of ovarian tissues (specifically targeting the stroma, cortical follicles, and post-ovulatory follicles) is planned to diagnose morphologically potential atresia rates, quantify the follicular reserve, and verify the structural remodeling predicted by our transcriptomic data (such as *MMP13* activation). Future studies will also necessitate expanding the sample size to enhance the representativeness of the cohorts, thereby minimizing individual biological variability and bolstering the statistical power of our conclusions. Ultimately, this integrated, multi-disciplinary approach will be required to clarify and validate the mechanisms driving the duration and intensity of the egg-laying plateau in poultry.

Supplementary Materials: The following supporting information can be downloaded at https://www.mdpi.com/article/10.3390/poultry5060077/s1, Figure S1: Gene Ontology (GO) functional enrichment analysis of differentially expressed genes (DEGs) in the molecular function category; Figure S2: Network analysis of protein–protein interactions of DEGs in chicken follicle tissues; Table S1: Composition and nutritional value of the basal diet for Dekalb White laying hens across different age periods; Table S2: Zootechnical performance parameters of laying hens in the PP and DP groups; Table S3: Morphometric parameters of internal organs in laying hens of the PP and DP groups; Table S4: Morphological blood characteristics, cellular elements, and color index of laying hens in the PP and DP groups; Table S5: Innate resistance and phagocytic parameters in laying hens of the PP and DP groups; Table S6: Total protein concentration and serum protein fractions in laying hens of the PP and DP groups; Table S7: Biochemical status and mineral metabolism profiles in laying hens of the PP and DP groups.

Author Contributions: Conceptualization, G.Y.L., E.A.Y. and V.A.F.; methodology, O.A.M., P.V.G., E.P.G., V.A.F., E.A.B. and K.A.S.; software, E.A.B.; validation, V.A.F., K.A.S., V.A.Z., A.A.S. and D.K.G.; formal analysis, E.A.Y., E.A.B., V.A.K. and K.N.T.; investigation, E.P.G., D.G.T., L.A.I., K.A.S., P.V.G., A.Y.B., V.A.Z., A.A.S., V.A.K. and K.N.T.; resources, G.Y.L., D.G.T. and V.Y.M.; data curation, A.Y.B., E.A.B. and V.A.Z.; writing—original draft preparation, E.A.Y., O.A.M. and M.N.R.; writing—review and editing, D.G.T., D.K.G. and M.N.R.; visualization, E.A.B. and A.A.S.; supervision, G.Y.L., D.G.T., V.Y.M. and D.K.G.; project administration, L.A.I., G.Y.L., D.G.T. and M.N.R.; funding acquisition, G.Y.L. and V.Y.M. All authors have read and agreed to the published version of the manuscript.

Funding: This research was financially supported by the Russian Science Foundation, grant number 25-16-68017 (Extension 22-16-00128).

Institutional Review Board Statement: The animal study protocol was approved by the Bioethical Commission of the L.K. Ernst Federal Research Center for Animal Husbandry (Protocol No. 2025-01/1, dated 15 January 2025).

Informed Consent Statement: Informed consent was obtained from farm owner included in the study.

Data Availability Statement: The high-throughput sequencing data generated during this study have been deposited in the NCBI Sequence Read Archive (SRA) repository under BioProject ID PRJNA1454096 (http://www.ncbi.nlm.nih.gov/bioproject/1454096 accessed on 21 September 2026). The individual biological replicates are available under BioSample accession numbers SAMN57292529–SAMN57292531 for the early-persistent production (PP) group and SAMN57292532–SAMN57292534 for the late-degraded production (DP) group.

Acknowledgments: During the preparation of this manuscript, the authors utilized Google Gemini models (September 2026; Google LLC, Mountain View, CA, USA) for English language support, specifically for reference formatting, text translation, and editorial refinement to improve the clarity and grammar of the draft from the original Russian manuscript and during the integration of Russian-language text sources. The authors confirm that these AI tools were not used for generating scientific content, data analysis, or the interpretation of results. All scientific ideas, data, and conclusions

remain the sole responsibility of the authors. The authors have thoroughly reviewed and edited the output and accept full responsibility for the final content of this publication.

Conflicts of Interest: The authors declare no conflicts of interest. Specifically, the authors affirm that they had no financial motivation to present positive data regarding the efficacy of any product reported in this paper. Some of the co-authors (Elena A. Yildirim, Elena P. Gorfunkel, Georgi Yu. Laptev, Daria G. Tiurina, Valentina A. Filippova, Larisa A. Ilina, Kseniya A. Sokolova, Vasiliy A. Zaikin, Alesya A. Savicheva, Valeria A. Kalmykova, Ksenia N. Timofeeva, Polina V. Grek, and Alexandra Y. Burlakova) are employed by BIOTROF+ Ltd. Additionally, co-authors Elena P. Gorfunkel, Georgi Yu. Laptev, Valentina A. Filippova, Larisa A. Ilina, and Polina V. Grek received a research grant from the Russian Science Foundation (Grant No. 22-16-00128-P). The funders had no role in the design of the study; in the collection, analyses, or interpretation of data; in the writing of the manuscript; or in the decision to publish the results. The remaining authors declare that the research was conducted in the absence of any commercial or financial relationships that could be construed as a potential conflict of interest.

Abbreviations

The following abbreviations are used in this manuscript:

ALB	Albumin
ALP	Alkaline phosphatase
ANOVA	Analysis of variance
AvBD4	Avian beta-defensin 4
bHLH	Basic helix–loop–helix
CCR2	C-C motif chemokine receptor 2
CPLX1	Complexin 1
CYP11A1	Cytochrome P450 family 11 subfamily A member 1
DEGs	Differentially expressed genes
DGE	Differential gene expression
DP	Degraded production (plateau) group
ECM	Extracellular matrix
FC	Fold change
FGF12	Fibroblast growth factor 12
FHAD1	Forkhead associated phosphopeptide binding domain 1
GABRA1	Gamma-aminobutyric acid type A receptor alpha1 subunit
GC	Guanine and cytosine content
GO	Gene ontology
GSEA	Gene set enrichment analysis
HSPB9	Heat shock protein family B (small) member 9
ID2	Inhibitor of DNA binding 2, HLH protein
IFNLR1	Interferon lambda receptor 1
IgG	Immunoglobulin G
IHH	Indian hedgehog
LY86	Lymphocyte antigen 86
LYG3	Lysozyme g3
MCC	Maximum Clique Centrality
MMP10	Matrix metallopeptidase 10
MMP13	Matrix metalloproteinase 13
MMPs	Matrix metalloproteinases
NC	Normalized count
NDUFAB1	NADH:ubiquinone oxidoreductase subunit AB1
NES	Normalized enrichment score
PC1	First principal component
PC2	Second principal component
PCA	Principal component analysis

PCV	Packed cell volume (hematocrit)
PDCL2	Phosducin like 2
PLTP	Phospholipid transfer protein
PNLIPRP1	Pancreatic lipase related protein 1
PP	Persistent production (plateau) group
RNA-Seq	RNA sequencing
SBA	Serum bactericidal activity
SEM	Standard error of the mean
SERPINB10B	Serpin peptidase inhibitor, clade B (ovalbumin), member 10 B
SERPINB14	Ovalbumin, or *OVAL*
SERPINB14B	Ovalbumin-related Y, or *OVAY*
SERPINB14C	Ovalbumin-related X, or *OVAX*
SFRP5	Secreted frizzled related protein 5
STAR	Spliced Transcripts Alignment to a Reference
STAR	Steroidogenic acute regulatory protein
TLR1A	Toll like receptor 16
TLR2A	Toll like receptor 2A
TLR4	Toll like receptor 4
TLR7	Toll like receptor 7
VLDL	Very-low-density lipoprotein
WNT4	Wnt family member 4
WNT5B	Wnt family member 5B

References

1. Gianfredi, V.; Nucci, D.; Pennisi, F.; Maggi, S.; Veronese, N.; Soysal, P. Aging, longevity, and healthy aging: The public health approach. *Aging Clin. Exp. Res.* **2025**, *37*, 125. [CrossRef] [PubMed]
2. Gržinić, G.; Piotrowicz-Cieślak, A.; Klimkowicz-Pawlas, A.; Górny, R.L.; Ławniczek-Wałczyk, A.; Piechowicz, L.; Olkowska, E.; Potrykus, M.; Tankiewicz, M.; Krupka, M.; et al. Intensive poultry farming: A review of the impact on the environment and human health. *Sci. Total Environ.* **2023**, *858*, 160014. [CrossRef] [PubMed]
3. Yuan, R.; Hascup, E.; Hascup, K.; Bartke, A. Relationships among development, growth, body size, reproduction, aging, and longevity–trade-offs and pace-of-life. *Biochemistry* **2023**, *88*, 1692–1703. [CrossRef] [PubMed]
4. El-Sabrout, K.; Aggag, S.; Mishra, B. Advanced practical strategies to enhance table egg production. *Scientifica* **2022**, *2022*, 1393392. [CrossRef] [PubMed]
5. Kochish, I.I.; Romanov, M.N.; Nikonov, I.N.; Ilyina, L.A.; Laptev, G.Y. Determination of Intestinal Microbiocenoses in Hens of Egg-type Crosses. In *World and Russian Trends in the Development of Poultry Industry: The Realities and Challenges of the Future, Proceedings of the 19th International Conference, Sergiyev Posad, Russia, 15–17 May 2018*; Fisinin, V.I., Ed.; World's Poultry Science Association (WSPA) Russian Branch, All-Russian Poultry Research and Technological Institute: Sergiyev Posad, Russia, 2018; pp. 240–243. Available online: https://kar.kent.ac.uk/89487/ (accessed on 21 September 2026).
6. Moiseeva, I.; Tolokonnikova, E. Effect of crossbreeding on egg quality in the progeny. *Ptitsevodstvo* **1973**, *3*, 28–30.
7. Raetskii, A.V.; Mamontova, I.; Moiseeva, I. Results of using Moscow chickens of M5 line for crossing with White Leghorns of Highsex cross. *Izv. Timiryazevsk. S-Kh. Akad.* **1981**, *6*, 136–142.
8. Bondarenko, Y.V.; Rozhkovsky, A.V.; Romanov, M.N.; Bogatyr, V.P. The use of genetical systems in the development of autosex crosses of egg-laying chickens. *Ptitsevodstvo* **1989**, *42*, 11–14.
9. Khvostyk, V.; Tereshchenko, O.; Zakharchenko, O.; Bondarenko, Y. Influence of "adding blood" of cocks of foreign crosses upon economically beneficial attributes of meat-egg hens of domestic selection. *Visn. Agrarn. Nauk.* **2017**, *95*, 44–48. [CrossRef]
10. Kim, S. Challenges and constraints to the sustainability of poultry farming in Republic of Korea. *Anim. Biosci.* **2025**, *38*, 829–844. [CrossRef] [PubMed]
11. Widowski, T.M.; Cooley, L.; Hendriksen, S.; Peixoto, M.R. Maternal age and maternal environment affect egg composition, yolk testosterone, offspring growth and behaviour in laying hens. *Sci. Rep.* **2022**, *12*, 1828. [CrossRef] [PubMed]
12. Grossman, M.; Koops, W.J. A model for individual egg production in chickens. *Poult. Sci.* **2001**, *80*, 859–867. [CrossRef] [PubMed]
13. Wolc, A.; Arango, J.; Fulton, J.E. Genetics and genomics of egg production traits in poultry species. In *Advances in Poultry Genetics and Genomics*; Aggrey, S.E., Zhou, H., Tixier-Boichard, M., Rhoads, D.D., Eds.; Burleigh Dodds Science Publishing: Cambridge, UK, 2020; pp. 151–182. [CrossRef]

14. Kuhnlein, U.; Aggrey, S.E.; Kansaku, N.; Zadworny, D. DNA polymorphisms in functional genes. In *Poultry Genetics, Breeding and Biotechnology*; Muir, W.M., Aggrey, S.E., Eds.; CAB International: Wallingford, UK; Cambridge, UK, 2003; pp. 647–663. [CrossRef]
15. Arthur, J.A.; Albers, G.A. Industrial perspective on problems and issues associated with poultry breeding. In *Poultry Genetics, Breeding and Biotechnology*; Muir, W.M., Aggrey, S.E., Eds.; CAB International: Wallingford, UK; Cambridge, UK, 2003; pp. 1–12. [CrossRef]
16. Preisinger, R.; Flock, D.K. Changes in genetic parameters and genetic progress in layers during two decades of intensive selection. In *Book of Abstracts of the 49th Annual Meeting of the European Association for Animal Production*; van Arendonk, J.A.M., Ed.; Wageningen Academic Publishers: Wageningen, The Netherlands, 1998; p. 38. [CrossRef] [PubMed]
17. Decuypere, E.; Bruggeman, V.; Barbato, G.F.; Buyse, J. Growth and reproduction problems associated with selection for increased broiler meat production. In *Poultry Genetics, Breeding and Biotechnology*; Muir, W.M., Aggrey, S.E., Eds.; CAB International: Wallingford, UK; Cambridge, UK, 2003; pp. 13–28. [CrossRef]
18. Arulnathan, V.; Turner, I.; Bamber, N.; Ferdous, J.; Grassauer, F.; Doyon, M.; Pelletier, N. A systematic review of potential productivity, egg quality, and animal welfare implications of extended lay cycles in commercial laying hens in Canada. *Poult. Sci.* **2024**, *103*, 103475. [CrossRef] [PubMed]
19. Kavtarashvili, A.S.; Golovkina, O.O.; Chekaleva, A.V. *Scientific Basis for Extending the Productive Life of Chickens*; Vologda Scientific Center of the Russian Academy of Sciences: Vologda, Russia, 2020. Available online: https://elibrary.ru/item.asp?id=45594178 (accessed on 21 September 2026).
20. Wadood, A.A.; Zhang, X. The omics revolution in understanding chicken reproduction: A comprehensive review. *Curr. Issues Mol. Biol.* **2024**, *46*, 6248–6266. [CrossRef] [PubMed]
21. Shcherbatov, V.I.; Shkuro, A.G. The cyclicity of laying eggs in chickens. *Coll. Sci. Pap. Krasn. Sci. Cent. Anim. Husb. Vet. Med.* **2020**, *9*, 113–117. [CrossRef]
22. Rebke, M.; Coulson, T.; Becker, P.H.; Vaupel, J.W. Reproductive improvement and senescence in a long-lived bird. *Proc. Natl. Acad. Sci. USA* **2010**, *107*, 7841–7846. [CrossRef] [PubMed]
23. Xu, J.; Li, R.; Liu, Y.; Wang, X.; Huang, K.; Zhao, Q.; Dessie, T.; Svitek, N.; Zhao, X.; Zhang, J.; et al. Dietary genistein supplementation enhances reproductive and bone health in late-laying hens. *Poult. Sci.* **2026**, *105*, 106554. [CrossRef] [PubMed]
24. Gao, Z.; Zheng, J.; Xu, G. Molecular mechanisms and regulatory factors governing feed utilization efficiency in laying hens: Insights for sustainable poultry production and breeding optimization. *Int. J. Mol. Sci.* **2025**, *26*, 6389. [CrossRef] [PubMed]
25. Gaviley, O.V.; Tereshchenko, O.V.; Artemenko, O.B.; Ogurtsova, N.S. Fertilizing capacity of spermatozoa of roosters in experimental T-2 toxicosis. *Ptakhivnytstvo* **2009**, *63*, 156–160.
26. Kutnyuk, P.I.; Kotik, A.I.; Trufanova, V.A.; Bondarenko, Y.V. A search for genetic-biological markers of resistance to mycotoxin T-2 in fowls. In *New Methods of Selection and Biotechnology in Animal Husbandry, Part 2. Reproduction, Population Genetics and Biotechnology*; Republican Production-Scientific Association for Implementation of Scientific and Technical Progress in Animal Husbandry: Kiev, Ukraine, 1991; pp. 108–109. Available online: https://www.cabidigitallibrary.org/doi/full/10.5555/19920198531 (accessed on 21 September 2026).
27. Laptev, G.Y.; Turina, D.G.; Yildirim, E.A.; Ilina, L.A.; Gorfunkel, E.P.; Filippova, V.A.; Dubrovin, A.V.; Melikidi, V.K.; Novikova, N.I.; Kalitkina, K.A.; et al. Analysis of changes in broiler microbiome biodiversity parameters due to intake of glyphosate and probiotic *Bacillus* sp. Gl-8 using next-generation sequencing. In *Agriculture Digitalization and Organic Production (ADOP 2023)*; Smart Innovation, Systems and Technologies; Ronzhin, A., Kostyaev, A., Eds.; Springer Nature: Singapore, 2023; Volume 362, pp. 161–170. [CrossRef]
28. Yildirim, E.A.; Laptev, G.Y.; Tiurina, D.G.; Gorfunkel, E.P.; Ilina, L.A.; Filippova, V.A.; Dubrovin, A.V.; Brazhnik, E.A.; Novikova, N.I.; Melikidi, V.K.; et al. Investigating adverse effects of chronic dietary exposure to herbicide glyphosate on zootechnical characteristics and clinical, biochemical and immunological blood parameters in broiler chickens. *Vet. Res. Commun.* **2024**, *48*, 153–164. [CrossRef] [PubMed]
29. Kochish, I.I.; Romanov, M.N.; Myasnikova, O.V.; Smolensky, V.I.; Martynov, V.V.; Nikonov, I.N.; Selina, M.V.; Kolesnikova, R.R.; Bernikova, K.E.; Motin, M.S. *Practical Recommendations for the Use of Feed Additives to Improve the Productivity and Stress Resistance of Egg Poultry*; Sel'skokhozyaistvennye Tekhnologii: Moscow, Russia, 2019. Available online: https://www.researchgate.net/publication/371539983 (accessed on 21 September 2026).
30. Kochish, I.I.; Romanov, M.N.; Myasnikova, O.V.; Nikonov, I.N.; Selina, M.V.; Korenyuga, M.V.; Zimin, E.E.; Sharafetdinov, G.R.; Martynov, V.V. *Methodical Recommendations on the Use of Antimicrobial Feed Additive for the Prevention of Stress in Industrial Crosses of Laying Hens*; Sel'skokhozyaistvennye Tekhnologii: Moscow, Russia, 2021. [CrossRef]
31. Ionov, I.A.; Gaviley, O.V.; Fotina, T.I.; Griffin, D.K.; Romanov, M.N. Brown mustard (*Brassica juncea* Czern) processing by-products: Effects of mustard meal xenobiotics on the productive performance and antioxidant system of laying hens. *Asian J. Agric. Rural Dev.* **2026**, *16*, 103–114. [CrossRef]
32. He, T.; Li, Y.; Huang, J.; Su, W.; Liu, S.; Quan, J.; Zhong, G.; Liu, Z.; Shi, D.; Yu, W. Boron triggers hepatic ferroptosis: Unveiling the dual-pathogenic nexus of oxidative stress and SLC7A11/GPX4 dysregulation. *Animals* **2026**, *16*, 832. [CrossRef] [PubMed]

33. Pan, J.; Liu, P.; Yu, X.; Zhang, Z.; Liu, J. The adverse role of endocrine disrupting chemicals in the reproductive system. *Front. Endocrinol.* **2024**, *14*, 1324993. [CrossRef] [PubMed]
34. Glatz, P.C.; Tilbrook, A.J. Welfare issues associated with moulting of laying hens. *Anim. Prod. Sci.* **2020**, *61*, 1006–1012. [CrossRef]
35. Zhang, L.; An, Z.; Li, W.; Liu, X.; Zhou, E.; Cui, P.; Zhang, Y.; Guo, Y.; Li, G.; Li, Z.; et al. Effect of induced molting on bone remodeling in laying hens. *BMC Genom.* **2025**, *26*, 1128. [CrossRef] [PubMed]
36. Wen, C.; Mai, C.; Cai, R.; Gou, Q.; Zhang, B.; Li, J.; Sun, C.; Yang, N. Inheritance of the duration of fertility in chickens and its correlation with laying performance. *Genet. Sel. Evol.* **2022**, *54*, 41. [CrossRef] [PubMed]
37. Dunn, I.C.; Miao, Y.-W.; Morris, A.; Romanov, M.N.; Wilson, P.W.; Waddington, D.; Sharp, P.J. Candidate genes and reproductive traits in a commercial broiler breeder population, an association study. *J. Anim. Sci.* **2001**, *79*, 43.
38. Kutnyuk, P.I.; Bondarenko, Y.V.; Ivanova, T.V. Karyometric method of determining the genetic potential of laying hens. *Ptakhivnytstvo* **2001**, *50*, 75–81.
39. Gadyuchko, O.T.; Sakhatsky, N.I.; Tereshchenko, A.V.; Anisimov, V.I.; Kislaya, E.D.; Svinarev, V.F. Genetic potential of breeds and populations of geese in Ukraine. *Ptakhivnytstvo* **2003**, *53*, 54–62.
40. Romanov, M.N.; Weigend, S. Genetic Diversity in Chicken Populations Based on Microsatellite Markers. In *Proceedings of the Conference "From Jay Lush to Genomics: Visions for Animal Breeding and Genetics"*; Dekkers, J.C.M., Lamont, S.J., Rothschild, M.F., Eds.; Iowa State University, Department of Animal Science: Ames, IA, USA, 1999; p. 174. Available online: https://kar.kent.ac.uk/46420/ (accessed on 21 September 2026).
41. Volkova, N.A.; Romanov, M.N.; Dzhagaev, A.Y.; Larionova, P.V.; Volkova, L.A.; Abdelmanova, A.S.; Vetokh, A.N.; Griffin, D.K.; Zinovieva, N.A. Genome-wide association studies and candidate genes for egg production traits in layers from an F_2 crossbred population produced using two divergently selected chicken breeds, Russian White and Cornish White. *Genes* **2025**, *16*, 583. [CrossRef] [PubMed]
42. Volkova, N.A.; Romanov, M.N.; Larionova, P.V.; Dzhagaev, A.Y.; Volkova, L.A.; Sermyagin, A.A.; Griffin, D.K.; Zinovieva, N.A. Genome-wide egg hunt: Unhiding candidate genes for egg component traits in layers of an F_2 resource population. *Animals* **2025**, *15*, 3391. [CrossRef] [PubMed]
43. Wu, N.; Zhu, Q.; Chen, B.; Gao, J.; Xu, Z.; Li, D. High-throughput sequencing of pituitary and hypothalamic microRNA transcriptome associated with high rate of egg production. *BMC Genom.* **2017**, *18*, 255. [CrossRef] [PubMed]
44. Chen, X.; Sun, X.; Chimbaka, I.M.; Qin, N.; Xu, X.; Liswaniso, S.; Xu, R.; Gonzalez, J.M. Transcriptome analysis of ovarian follicles reveals potential pivotal genes associated with increased and decreased rates of chicken egg production. *Front. Genet.* **2021**, *12*, 622751. [CrossRef] [PubMed]
45. Hendrix Genetics. *Dekalb White*; Hendrix Genetics BV: Boxmeer, The Netherlands, 2026. Available online: https://layinghens.hendrix-genetics.com/en/market/deutschland/dekalb-white-du/ (accessed on 21 September 2026).
46. Kochish, I.I.; Smolensky, V.I.; Laptev, G.Y.; Romanov, M.N.; Nikonov, I.N.; Panin, A.N.; Surai, P.F.; Ilyina, L.A.; Myasnikova, O.V.; Selina, M.V.; et al. *Methodical Recommendations on the Implementation of the Developed System for the Prevention of Pathogen Bacteria by Correcting Diets in Laying Hens and Using Antimicrobial Additives*; Sel'skokhozyaistvennye Tekhnologii: Moscow, Russia, 2018. Available online: https://kar.kent.ac.uk/75283/ (accessed on 21 September 2026).
47. Kochish, I.I.; Surai, P.F.; Romanov, M.N.; Smolensky, V.I.; Nikonov, I.N.; Selina, M.V.; Myasnikova, O.V.; Kolesnikova, R.R. *Methodical Recommendations on the Application of the Foundations of the Technology of Feeding Egg-Type Chickens, Providing a High Percentage of Realization of Their Genetic Potential for Productivity*; Sel'skokhozyaistvennye Tekhnologii: Moscow, Russia, 2019. Available online: https://elibrasry.ru/item.asp?id=41589562 (accessed on 21 September 2026).
48. Kochish, I.I.; Yildirim, E.A.; Laptev, G.Y.; Ilina, L.A.; Tyurina, D.G.; Dubrovin, A.V.; Filippova, V.A.; Novikova, N.I.; Tarlavin, N.V.; Romanov, M.N. *Guidelines for the Use of a Feed Additive Tested in an Industrial Environment on Highly Productive Commercial Laying Hens*; Sel'skokhozyaistvennye Tekhnologii: Moscow, Russia, 2020. Available online: https://kar.kent.ac.uk/89170/ (accessed on 21 September 2026).
49. Romanov, M.N.; Kochish, I.I.; Sharafetdinov, G.R.; Myasnikova, O.V.; Nikonov, I.N.; Selina, M.V.; Surai, P.F. Towards Advanced Biotechnological Developments to Realize the Genetic Potential of Egg-type Poultry. In *Molecular Genetic Technologies for Analysis of Gene Expression Related to Animal Productivity and Disease Resistance, Materials of the 3rd International Scientific and Practical Conference, Moscow, Russia, 30 September 2021*; Pozyabin, S.V., Kochish, I.I., Romanov, M.N., Gnezdilova, L.A., Surai, P.F., Nikonov, I.N., Selina, M.V., Eds.; Sel'skokhozyaistvennye Tekhnologii: Moscow, Russia, 2021; pp. 40–51. [CrossRef]
50. Antonov, V.M.; Yakubovskaya, S.N.; Nachalnaya, Z.P.; Romanov, M.N. (Eds.) *Technology of Growing Chickens and Geese*; Information Bulletin, No. 1; Ukrainian Poultry Research Institute: Kharkov, USSR, 1991. Available online: https://kar.kent.ac.uk/106938/ (accessed on 21 September 2026).
51. Karpenko, L.Y.; Bakhta, A.A.; Babich, O.O.; Sukhikh, S.A.; Vorobyov, N.I.; Nikonov, I.N.; Borisova, S.D.; Griffin, D.K.; Romanov, M.N. Effects of a complex feed additive on productivity and blood parameters of laying hens using stochastic fractal-based neural network model. *Poult. Sci. J.* **2025**, *13*, 243–252. [CrossRef]

52. Da Nóbrega, I.P.T.; Reis, M.d.P.; Morillo, F.A.H.; De Freitas, L.F.V.-B.; Bittencourt, L.C.; Fernandes, J.B.K.; Sakomura, N.K. Dynamics of growth and egg traits in three dietary balanced protein scenarios applied for laying hens. *Animals* **2022**, *12*, 1371. [CrossRef] [PubMed]
53. Moiseyeva, I.G.; Bannikova, L.V.; Altukhov, Y.P. State of poultry breeding in Russia: Genetic monitoring. *Mezhdunar. Sel'skokhoz. Zh.* **1993**, *5–6*, 66–69.
54. Zakharov-Gesekhus, I.A.; Stolpovsky, Y.A.; Ukhanov, S.V.; Moiseyeva, I.G.; Sulimova, G.E. Monitoring the gene pools of animal populations in connection with selection tasks and the study of phylogeny. In *Farm Animals*; Russian Academy of Sciences: Moscow, Russia, 2007; pp. 122–124.
55. Shomina, N.V.; Tkachenko, S.M.; Tagirov, M.T.; Tereshchenko, O.V. Monitoring the quality of hatching eggs during storage. *Ef. Ptakhivnytstvo* **2009**, *11*, 29–33.
56. Chen, Z.; Wen, D. Ovarian transcriptome profile from egg-laying period to incubation period of Changshun green-shell laying hens. *Genes* **2025**, *16*, 394. [CrossRef] [PubMed]
57. Leary, S.; Underwood, W.; Anthony, R.; Cartner, S.; Grandin, T.; Greenacre, C.; Gwaltney-Brant, S.; McCrackin, M.A.; Meyer, R.; Miller, D.; et al. (Eds.) *AVMA Guidelines for the Euthanasia of Animals: 2020 Edition*; American Veterinary Medical Association: Schaumburg, IL, USA, 2020. Available online: https://www.spandidos-publications.com/var/AVMA_euthanasia_guidelines_2020.pdf (accessed on 21 September 2026).
58. Chung, J.Y.; Braunschweig, T.; Williams, R.; Guerrero, N.; Hoffmann, K.M.; Kwon, M.; Song, Y.K.; Libutti, S.K.; Hewitt, S.M. Factors in tissue handling and processing that impact RNA obtained from formalin-fixed, paraffin-embedded tissue. *J. Histochem. Cytochem.* **2008**, *56*, 1033–1042. [CrossRef] [PubMed]
59. Chen, Q.; Wang, Y.; Liu, Z.; Guo, X.; Sun, Y.; Kang, L.; Jiang, Y. Transcriptomic and proteomic analyses of ovarian follicles reveal the role of VLDLR in chicken follicle selection. *BMC Genom.* **2020**, *21*, 486. [CrossRef] [PubMed]
60. Komatsu, K.; Masubuchi, S. Observation of the dynamics of follicular development in the ovary. *Reprod. Med. Biol.* **2017**, *16*, 21–27. [CrossRef] [PubMed]
61. Cavalcanti, G.S.; Carvalho, K.C.; Ferreira, C.d.S.; Alvarez, P.A.C.; Monteleone, P.A.A.; Baracat, E.C.; Soares Júnior, J.M. Granulosa cells and follicular development: A brief review. *Rev. Assoc. Med. Bras.* **2023**, *69*, e20230175. [CrossRef] [PubMed]
62. Shen, L.; Liu, J.; Luo, A.; Wang, S. The stromal microenvironment and ovarian aging: Mechanisms and therapeutic opportunities. *J. Ovarian Res.* **2023**, *16*, 237. [CrossRef] [PubMed]
63. Kushaliev, K.Z. *Necropsy and Pathomorphological Diagnosis of Animal and Poultry Diseases*; Zhangir Khan West Kazakhstan Agricultural-Technical University: Uralsk, Kazakhstan, 2023.
64. Tietz, N.W. *Encyclopedia of Clinical Laboratory Tests*; Menshikov, V.V., Ed.; Labinform Publishing House: Moscow, Russia, 1997. Available online: https://clinlabs.com/books/enciklopediya-klinicheskih-laboratornyh-testov (accessed on 21 September 2026).
65. Kostyna, M.A. Determination of classes of immunoglobulins by the method of discrete sedimentation. In *Problems of Increasing the Resistance of Newborn Animals: Collection of Scientific Papers of VNIINBZh*; VNIINBZh: Voronezh, Ukraine, 1983; pp. 76–80.
66. Menshikov, V.V. *Clinical Diagnosis—Laboratory Basics*; Labinform Publishing House: Moscow, Russia, 1997. Available online: http://clinlab.ru/main/books/labinf/book3.htm (accessed on 21 September 2026).
67. Filippova, V.A.; Laptev, G.Y.; Ilina, L.A.; Yildirim, E.A.; Ponomareva, E.S.; Brazhnik, E.A.; Novikova, N.I.; Tiurina, D.G.; Dubrovin, A.V.; Sokolova, K.A.; et al. Comparative genomics of two novel *Bacillus* strains: Microbiomic insights into the sequences, metabolomics, and potential safe use in the creation of biopreparations. *Front. Biosci. Elite Ed.* **2025**, *17*, 28227. [CrossRef] [PubMed]
68. Yildirim, E.A.; Laptev, G.Y.; Tiurina, D.G.; Filippova, V.A.; Ilina, L.A.; Novikova, N.I.; Sokolova, K.A.; Ponomareva, E.S.; Zaikin, V.A.; Klyuchnikova, I.A.; et al. Comparison of the endometrial microbiome of cows under eco-farm conditions in the early and late dry periods. *Anim. Husb. Fodd. Prod.* **2025**, *108*, 21–35. [CrossRef]
69. Yildirim, E.A.; Laptev, G.Y.; Tiurina, D.G.; Filippova, V.A.; Ilina, L.A.; Novikova, N.I.; Sokolova, K.A.; Patiukova, N.S.; Klyuchnikova, I.A.; Savicheva, A.A.; et al. Bioinformatics Analysis of the Genome of *E. faecalis* E-10 Strain Isolated from Cow Endometrium. In *Biologization and Sustainable Development of Agriculture: Proceedings of the Sixth International Conference on Agriculture Digitalization and Organic Production (ADOP 2026), Kaliningrad, Russia, 1–5 June 2026*; Smart Innovation, Systems and Technologies; Ronzhin, A., Ogiy, O., Surovtsev, V., Eds.; Springer: Cham, Switzerland, 2026; Volume 8771, pp. 230–238. [CrossRef]
70. Romanov, M.N.; Shakhin, A.V.; Abdelmanova, A.S.; Volkova, N.A.; Efimov, D.N.; Fisinin, V.I.; Korshunova, L.G.; Anshakov, D.V.; Dotsev, A.V.; Griffin, D.K.; et al. Dissecting selective signatures and candidate genes in grandparent lines subject to high selection pressure for broiler production and in a local Russian chicken breed of Ushanka. *Genes* **2024**, *15*, 524. [CrossRef] [PubMed]
71. Volkova, N.A.; German, N.Y.; Larionova, P.V.; Vetokh, A.N.; Romanov, M.N.; Zinovieva, N.A. Identification of SNPs and candidate genes associated with abdominal fat deposition in quails (*Coturnix japonica*). *Sel'skokhoz. Biol.* **2023**, *58*, 1079–1087. [CrossRef]
72. Volkova, N.A.; Romanov, M.N.; Abdelmanova, A.S.; Larionova, P.V.; German, N.Y.; Vetokh, A.N.; Shakhin, A.V.; Volkova, L.A.; Anshakov, D.V.; Fisinin, V.I.; et al. Genotyping-by-sequencing strategy for integrating genomic structure, diversity and performance of various Japanese quail (*Coturnix japonica*) breeds. *Animals* **2023**, *13*, 3439. [CrossRef] [PubMed]

73. Ewels, P.; Magnusson, M.; Lundin, S.; Käller, M. MultiQC: Summarize analysis results for multiple tools and samples in a single report. *Bioinformatics* **2016**, *32*, 3047–3048. [CrossRef] [PubMed]
74. Bolger, A.M.; Lohse, M.; Usadel, B. Trimmomatic: A flexible trimmer for Illumina sequence data. *Bioinformatics* **2014**, *30*, 2114–2120. [CrossRef] [PubMed]
75. Kim, D.; Paggi, J.M.; Park, C.; Bennett, C.; Salzberg, S.L. Graph-based genome alignment and genotyping with HISAT2 and HISAT-genotype. *Nat. Biotechnol.* **2019**, *37*, 907–915. [CrossRef] [PubMed]
76. Abdelmanova, A.S.; Shakhin, A.V.; Romanov, M.N.; Korshunova, L.G.; Emanuilova, Z.V. Evaluation of genetic differentiation of chicken lines used for breeding meat crosses. *Izv. St.-Petersburg State Agrar. Univ.* **2024**, *78*, 87–95. [CrossRef]
77. Romanov, M.N.; Sazanov, A.A.; Moiseyeva, I.; Smirnov, A.F. Poultry. In *Genome Mapping and Genomics in Animals*; Volume 3: Genome Mapping and Genomics in Domestic Animals; Cockett, N.E., Kole, C., Eds.; Springer: Berlin/Heidelberg, Germany; New York, NY, USA, 2009; pp. 75–141. [CrossRef]
78. Dobin, A.; Davis, C.A.; Schlesinger, F.; Drenkow, J.; Zaleski, C.; Jha, S.; Batut, P.; Chaisson, M.; Gingeras, T.R. STAR: Ultrafast universal RNA-seq aligner. *Bioinformatics* **2013**, *29*, 15–21. [CrossRef] [PubMed]
79. Love, M.I.; Huber, W.; Anders, S. Moderated estimation of fold change and dispersion for RNA-seq data with DESeq2. *Genome Biol.* **2014**, *15*, 550. [CrossRef] [PubMed]
80. Kleverov, M.; Zenkova, D.; Kamenev, V.; Sablina, M.; Artyomov, M.N.; Sergushichev, A.A. Phantasus, a web application for visual and interactive gene expression analysis. *eLife* **2024**, *13*, e85722. [CrossRef] [PubMed]
81. McCarthy, D.J.; Chen, Y.; Smyth, G.K. Differential expression analysis of multifactor RNA-Seq experiments with respect to biological variation. *Nucleic Acids Res.* **2012**, *40*, 4288–4297. [CrossRef] [PubMed]
82. Zhu, A.; Ibrahim, J.G.; Love, M.I. Heavy-tailed prior distributions for sequence count data: Removing the noise and preserving large differences. *Bioinformatics* **2019**, *35*, 2084–2092. [CrossRef] [PubMed]
83. Reyer, H.; Oster, M.; Zentek, J.; Männer, K.; Trakooljul, N.; Aumiller, T.; Wimmers, K. Digestibility and transcriptomic profiling of kidney, pancreas, follicle, and uterus in laying hens supplemented with phytogenic feed additive. *Poult. Sci.* **2026**, *105*, 106219. [CrossRef] [PubMed]
84. Murrell, P. *R Graphics*; Chapman and Hall/CRC: New York, NY, USA, 2005. [CrossRef]
85. Joly, J.H.; Lowry, W.E.; Graham, N.A. Differential Gene Set Enrichment Analysis: A statistical approach to quantify the relative enrichment of two gene sets. *Bioinformatics* **2020**, *36*, 5247–5254. [CrossRef] [PubMed]
86. Schurch, N.J.; Schofield, P.; Gierliński, M.; Cole, C.; Sherstnev, A.; Singh, V.; Wrobel, N.; Gharbi, K.; Simpson, G.G.; Owen-Hughes, T.; et al. How many biological replicates are needed in an RNA-seq experiment and which differential expression tool should you use? *RNA* **2016**, *22*, 839–851. [CrossRef] [PubMed]
87. Doncheva, N.T.; Morris, J.H.; Gorodkin, J.; Jensen, L.J. Cytoscape StringApp: Network analysis and visualization of proteomics data. *J. Proteome Res.* **2019**, *18*, 623–632. [CrossRef] [PubMed]
88. Shannon, P.; Markiel, A.; Ozier, O.; Baliga, N.S.; Wang, J.T.; Ramage, D.; Amin, N.; Schwikowski, B.; Ideker, T. Cytoscape: A software environment for integrated models of biomolecular interaction networks. *Genome Res.* **2003**, *13*, 2498–2504. [CrossRef] [PubMed]
89. Chin, C.H.; Chen, S.H.; Wu, H.H.; Ho, C.W.; Ko, M.T.; Lin, C.Y. cytoHubba: Identifying hub objects and sub-networks from complex interactome. *BMC Syst. Biol.* **2014**, *8*, S11. [CrossRef] [PubMed]
90. Bhattacharyya, N.; Khan, M.M.; Bagabir, S.A.; Almalki, A.H.; Shahwan, M.A.; Haque, S.; Verma, A.K.; Mangangcha, I.R. Maximal clique centrality and bottleneck genes as novel biomarkers in ovarian cancer. *Biotechnol. Genet. Eng. Rev.* **2023**, *39*, 1273–1296. [CrossRef] [PubMed]
91. Kochish, I.I.; Brazhnik, E.A.; Vorobyov, N.I.; Nikonov, I.N.; Korenyuga, M.V.; Myasnikova, O.V.; Griffin, D.K.; Surai, P.F.; Romanov, M.N. Features of fractal conformity and bioconsolidation in the early myogenesis gene expression and their relationship to the genetic diversity of chicken breeds. *Animals* **2023**, *13*, 521. [CrossRef] [PubMed]
92. Johnson, M.L. Nonlinear least-squares fitting methods. *Methods Cell Biol.* **2008**, *84*, 781–805. [CrossRef] [PubMed]
93. Meza Cerda, M.I.; Gray, R.; Higgins, D.P. Cytokine RT-qPCR and ddPCR for immunological investigations of the endangered Australian sea lion (*Neophoca cinerea*) and other mammals. *PeerJ* **2020**, *8*, e10306. [CrossRef] [PubMed]
94. Laptev, G.Y.; Filippova, V.A.; Kochish, I.I.; Yildirim, E.A.; Ilina, L.A.; Dubrovin, A.V.; Brazhnik, E.A.; Novikova, N.I.; Novikova, O.B.; Dmitrieva, M.E.; et al. Examination of the expression of immunity genes and bacterial profiles in the caecum of growing chickens infected with *Salmonella* Enteritidis and fed a phytobiotic. *Animals* **2019**, *9*, 615. [CrossRef] [PubMed]
95. Livak, K.J.; Schmittgen, T.D. Analysis of relative gene expression data using real-time quantitative PCR and the $2^{-\Delta\Delta CT}$ method. *Methods* **2001**, *25*, 402–408. [CrossRef] [PubMed]
96. Kondrakhin, I.P.; Arkhipov, A.V.; Levchenko, V.I. *Methods of Veterinary Clinical Laboratory Diagnostics: Handbook*; Kondrakhin, I.P., Ed.; KolosS: Moscow, Russia, 2004; 520p.

97. Scherf, B.D. (Ed.) *World Watch List for Domestic Animal Diversity*, 2nd ed.; Food and Agriculture Organization of the United Nations: Rome, Italy, 1995. Available online: https://web.archive.org/web/20151126034309/http://www.fao.org/ag/againfo/programmes/en/lead/toolbox/Indust/wwl.pdf (accessed on 21 September 2026).
98. El Fouikar, S.; Van Acker, N.; Héliès, V.; Frenois, F.X.; Giton, F.; Gayrard, V.; Dauwe, Y.; Mselli-Lakhal, L.; Rousseau-Ralliard, D.; Fournier, N.; et al. Folliculogenesis and steroidogenesis alterations after chronic exposure to a human-relevant mixture of environmental toxicants spare the ovarian reserve in the rabbit model. *J. Ovarian Res.* **2024**, *17*, 134. [CrossRef] [PubMed]
99. Leśniak-Walentyn, A.; Hrabia, A. Expression and localization of matrix metalloproteinases (MMP-2,-7,-9) and their tissue inhibitors (TIMP-2,-3) in the chicken oviduct during maturation. *Cell Tissue Res.* **2016**, *364*, 185–197. [CrossRef] [PubMed]
100. Wu, J.; Yan, Y.; Chen, J.; Li, J.; Li, G.; Wu, G.; Zheng, G.; Yang, Y.; Du, Y.; Lian, L. Transcriptome of the ovaries and oviduct associates inflammatory response with high blood and meat spots incidence in chickens. *BMC Genom.* **2025**, *26*, 1021. [CrossRef] [PubMed]
101. Yang, Q.; Lu, X.; Li, G.; Zhang, H.; Zhou, C.; Yin, J.; Han, W.; Yang, H. Genetic analysis of egg production traits in Luhua Chickens: Insights from a multi-trait animal model and a genome-wide association study. *Genes* **2024**, *15*, 796. [CrossRef] [PubMed]
102. Rozhkovsky, A.V.; Bondarenko, Y.V. Use of signal genes in obtaining promising hybrid combinations of egg-laying hens. *Nauch.-Tekh. Byull. Ukr. Nauch.-Issled. Inst. Ptitsevod.* **1984**, *17*, 3–6.
103. Moiseyeva, I.G. Native breeds of domestic fowl. In *Farm Animal Genetic Resources: Rare and Endangered Native Breeds*; Moiseyeva, I.G., Zakharov, I.A., Mitichashvili, R.S., Eds.; Nauka: Moscow, Russia, 1992; pp. 11–112. Available online: https://agris.fao.org/search/en/providers/122621/records/647396783ed73003714cc15a (accessed on 21 September 2026).
104. Jones, A.; Bernabé, B.P.; Padmanabhan, V.; Li, J.; Shikanov, A. Capitalizing on transcriptome profiling to optimize and identify targets for promoting early murine folliculogenesis in vitro. *Sci. Rep.* **2021**, *11*, 12517. [CrossRef] [PubMed]
105. Gruber, M.; Bos, E.S.; Ab, G. Hormonal control of vitellogenin synthesis in avian liver. *Mol. Cell Endocrinol.* **1976**, *5*, 41–50. [CrossRef] [PubMed]
106. Xie, Y.; Lin, L.; Sun, C.; Chen, L.; Lv, W. Association between serum alkaline phosphatase and clinical prognosis in patients with acute liver failure following cardiac arrest: A retrospective cohort study. *Eur. J. Med. Res.* **2024**, *29*, 453. [CrossRef] [PubMed]
107. Zhou, Y.; Xu, H.; Du, W.; Lu, Y.; Hu, Z.; Deng, Q.; Wang, X.; Liu, Y.; Zhang, Y.; Wang, Y. Impact of comb type on production performance, egg production quality, reproductive performance, and blood biochemical indexes in Tianfu chickens. *Poult. Sci.* **2025**, *104*, 104471. [CrossRef] [PubMed]
108. Suprapti, E.; Hadju, V.; Ibrahim, E.; Indriasari, R.; Erika, K.A.; Balqis, B. Anemia: Etiology, pathophysiology, impact, and prevention: A review. *Iran. J. Public Health* **2025**, *54*, 509–520. [CrossRef] [PubMed]
109. Cowieson, A.J.; Reisinger, N.; Milanese, A.; McCormack, U.M.; Phillips, C.A. Blood acid/base balance in poultry: Dietary, environmental, and physiological determinants and emerging diagnostic opportunities. *Poult. Sci.* **2026**, *105*, 107337. [CrossRef] [PubMed]
110. Muckenthaler, M.U.; Rodrigues, P.; Macedo, M.G.; Minana, B.; Brennan, K.; Cardoso, E.M.; Hentze, M.W.; de Sousa, M. Molecular analysis of iron overload in beta2-microglobulin-deficient mice. *Blood Cells Mol. Dis.* **2004**, *33*, 125–131. [CrossRef] [PubMed]
111. Green, M.R.; Sambrook, J. Alkaline Phosphatase. *Cold Spring Harb. Protoc.* **2020**, *2020*, 100768. [CrossRef] [PubMed]
112. Akbarian, S.; Sheikhi, M.; Khedri, P.; Baharifar, N.; Khalaf Shamsabadi, F.; Davidi, M.R.; Khazaei, H.A.; Assarian, H.; Sheikhi, A. The correlation between humoral immune responses and severity of clinical symptoms in COVID-19 patients. *Epidemiol. Infect.* **2023**, *151*, e158. [CrossRef] [PubMed]
113. Carroll, M.C. The role of complement and complement receptors in induction and regulation of immunity. *Annu. Rev. Immunol.* **1998**, *16*, 545–568. [CrossRef] [PubMed]
114. Qiu, Z.; Jiang, R.; Wu, S.; Zhan, R.; Hu, X.; Wang, S. Enlarged splenic volume predicts poor survival and is associated with inflammatory imbalance in patients with diffuse large B-cell lymphoma. *Blood Res.* **2026**, *61*, 28. [CrossRef] [PubMed]
115. Jarczak, D.; Nierhaus, A. Cytokine storm—Definition, causes, and implications. *Int. J. Mol. Sci.* **2022**, *23*, 11740. [CrossRef] [PubMed]
116. Conesa, A.; Madrigal, P.; Tarazona, S.; Gomez-Cabrero, D.; Cervera, A.; McPherson, A.; Szcześniak, M.W.; Gaffney, D.J.; Elo, L.L.; Zhang, X.; et al. A survey of best practices for RNA-seq data analysis. *Genome Biol.* **2016**, *17*, 13. [CrossRef] [PubMed]
117. SEQC/MAQC-III Consortium. A comprehensive assessment of RNA-seq accuracy, reproducibility and information content by the Sequencing Quality Control Consortium. *Nat. Biotechnol.* **2014**, *32*, 903–914. [CrossRef] [PubMed]
118. Deschamps-Francoeur, G.; Simoneau, J.; Scott, M.S. Handling multi-mapped reads in RNA-seq. *Comput. Struct. Biotechnol. J.* **2020**, *18*, 1569–1576. [CrossRef] [PubMed]
119. Rao, Y.S.; Chai, X.W.; Wang, Z.F.; Nie, Q.H.; Zhang, X.Q. Impact of GC content on gene expression pattern in chicken. *Genet. Sel. Evol.* **2013**, *45*, 9. [CrossRef] [PubMed]
120. Yao, F.; Coquery, J.; Lê Cao, K.A. Independent Principal Component Analysis for biologically meaningful dimension reduction of large biological data sets. *BMC Bioinform.* **2012**, *13*, 24. [CrossRef] [PubMed]

121. Koch, C.M.; Chiu, S.F.; Akbarpour, M.; Bharat, A.; Ridge, K.M.; Bartom, E.T.; Winter, D.R. A beginner's guide to analysis of RNA sequencing data. *Am. J. Respir. Cell Mol. Biol.* **2018**, *59*, 145–157. [CrossRef] [PubMed]
122. Rosati, D.; Palmieri, M.; Brunelli, G.; Morrione, A.; Iannelli, F.; Frullanti, E.; Giordano, A. Differential gene expression analysis pipelines and bioinformatic tools for the identification of specific biomarkers: A review. *Comput. Struct. Biotechnol. J.* **2024**, *23*, 1154–1168. [CrossRef] [PubMed]
123. Sun, M.; Wang, H.; Zhu, X.; Zhang, X.; Min, Y.; Ge, M.; Jiang, X.; Yu, W. The mechanism of egg production improvement in laying hens before and after molting revealed by transcriptome and metabolome integration. *Poult. Sci.* **2025**, *104*, 105125. [CrossRef] [PubMed]
124. Huang, T.; Fei, M.; Zhou, X.; He, K.; Yang, S.; Zhao, A. Effects of different photoperiods on the transcriptome of the ovary and small white follicles in Zhedong white geese. *Animals* **2024**, *14*, 2747. [CrossRef] [PubMed]
125. Adli, D.N.; Sugiharto, S.; Ujilestari, T.; Irawan, A.; Azmi, A.F.M.; Illaningtyas, F.; Wahyuni, D.S.; Qomariyah, N.; Sitaresmi, P.I.; Krisnan, R.; et al. Emulsifiers in poultry nutrition-molecular mechanism of lipid metabolism and energy utilization: A meta-analysis and KEGG mapping. *Poult. Sci.* **2026**, *105*, 106603. [CrossRef] [PubMed]
126. Tian, Y.; Wang, X.; Rao, Y.; Zhou, X.; Jiang, Y.; Liu, Q.; Wu, S.; Zhang, F. Identification and validation of differentially expressed genes in intramuscular fat metabolism in Guizhou yellow chickens using RNA-Seq analysis. *PLoS ONE* **2025**, *20*, e0326128. [CrossRef] [PubMed]
127. Tickle, P.G.; Hutchinson, J.R.; Codd, J.R. Energy allocation and behaviour in the growing broiler chicken. *Sci. Rep.* **2018**, *8*, 4562. [CrossRef] [PubMed]
128. Liao, Y.; Li, A.; Luo, Y.; Zhu, R.; Zhang, C.; Ma, M.; Li, Y.; Sun, L.; Shen, M.; Qu, L. Transcriptomic analysis reveals stage-specific cholesterol metabolism and steroidogenic in theca layer cells during follicular development in chickens. *Comp. Biochem. Physiol. D. Genom. Proteom.* **2026**, *57*, 101682. [CrossRef] [PubMed]
129. Zhou, Y.; Liu, J.; Lei, Q.; Han, H.; Liu, W.; Cunwei, T.; Li, F.; Cao, D. Transcriptome analysis of the chicken follicular theca cells with miR-135a-5p suppressed. *G3* **2020**, *10*, 4071–4081. [CrossRef] [PubMed]
130. Wang, J.; Wang, D.; Zhang, Y.; Sun, P.; Yi, L.; Han, A.; Zhao, W.; Zhang, Y.; Ma, H. Extracellular vesicles in reproductive biology and disorders: A comprehensive review. *Front. Endocrinol.* **2025**, *16*, 1550068. [CrossRef] [PubMed]
131. Li, J.; Liang, S.; Li, Y.; Wu, J.; Li, C.; Gan, J.; Li, W.; Wang, C. Immune dysregulation triggered by inflammatory cytokines in patients with severe respiratory infections. *Respir. Res.* **2026**, *27*, 53. [CrossRef] [PubMed]
132. Hu, W.N.; Jiao, W.J.; Ma, Z.; Dong, N.; Ma, Q.Q.; Shao, C.X.; Shan, A.S. The influence of isoleucine and arginine on biological activity and peptide-membrane interactions of antimicrobial peptides from the bactericidal domain of AvBD4. *Protein Pept. Lett.* **2013**, *20*, 1189–1199. [CrossRef] [PubMed]
133. Kochish, I.I.; Romanov, M.N.; Laptev, G.Y.; Yildirim, E.A.; Ilina, L.A.; Filippova, V.A.; Dubrovin, A.V.; Novikova, N.I.; Tyurina, D.G.; Tarlavin, N.V.; et al. *Methodological Recommendations for the Use of Modern Biotechnology for Assessing the Expression of Genes Associated with the Productivity and Resistance of Poultry to Adverse Factors*; Sel'skokhozyaistvennye Tekhnologii: Moscow, Russia, 2019. Available online: https://kar.kent.ac.uk/89338/ (accessed on 21 September 2026).
134. Laptev, G.Y.; Yildirim, E.A.; Ilina, L.A.; Filippova, V.A.; Kochish, I.I.; Gorfunkel, E.P.; Dubrovin, A.V.; Brazhnik, E.A.; Narushin, V.G.; Novikova, N.I.; et al. Effects of essential oils-based supplement and *Salmonella* infection on gene expression, blood parameters, cecal microbiome, and egg production in laying hens. *Animals* **2021**, *11*, 360. [CrossRef] [PubMed]
135. Naim, N.; Amrit, F.R.; McClendon, T.B.; Yanowitz, J.L.; Ghazi, A. The molecular tug of war between immunity and fertility: Emergence of conserved signaling pathways and regulatory mechanisms. *BioEssays* **2020**, *42*, e2000103. [CrossRef] [PubMed]
136. Hashim, P.H.; Perry, M.J.; Pritchard, M.T.; Gerton, J.L.; Duncan, F.E. Autonomous follicle quality control mechanisms: Innate immune signaling capabilities of granulosa cells. *Reproduction* **2025**, *169*, e250042. [CrossRef] [PubMed]
137. Wang, J.; Wang, G.J.; Wang, L.C.; Wang, L.L.; Qin, J.J.; Wang, B.; Cui, J.; Wu, H.L.; Li, R.; Liu, W. The mechanisms of energy balance between oxidative phosphorylation and glycolysis in human ovarian granulosa cells. *Front. Physiol.* **2026**, *17*, 1715312. [CrossRef] [PubMed]
138. Balakrishnan, K.N.; Ramiah, S.K.; Zulkifli, I. Heat shock protein response to stress in poultry: A review. *Animals* **2023**, *13*, 317. [CrossRef] [PubMed]
139. Ali, M.Y.; Faruque, S.; Ahmadi, S.; Ohkubo, T. Genetic analysis of *HSP70* and *HSF3* polymorphisms and their associations with the egg production traits of Bangladeshi hilly chickens. *Animals* **2024**, *14*, 3552. [CrossRef] [PubMed]
140. Kogut, M.H.; Chiang, H.I.; Swaggerty, C.L.; Pevzner, I.Y.; Zhou, H. Gene expression analysis of Toll-like receptor pathways in heterophils from genetic chicken lines that differ in their susceptibility to *Salmonella enteritidis*. *Front. Genet.* **2012**, *3*, 121. [CrossRef] [PubMed]
141. de Carvalho, L.M.; Carvalho, V.M.; Camargo, A.P.; Papes, F. Gene network analysis identifies dysregulated pathways in an autism spectrum disorder caused by mutations in Transcription Factor 4. *Sci. Rep.* **2025**, *15*, 4993. [CrossRef] [PubMed]
142. Sugimoto, Y.; Sanuki, S.; Ibrahim, H.R.; Aoki, T.; Kusakabe, T.; Koga, K. Occurrence of ovalbumin in ovarian yolk of chicken during oogenesis. *Biochim. Biophys. Acta* **2001**, *1526*, 1–4. [CrossRef] [PubMed]

143. Weerackoon, N.; Gunawardhana, K.L.; Mani, A. Wnt signaling cascades and their role in coronary artery health and disease. *J. Cell. Signal.* **2021**, *2*, 52. [CrossRef] [PubMed]
144. Love, M.I.; Hogenesch, J.B.; Irizarry, R.A. Modeling of RNA-seq fragment sequence bias reduces systematic errors in transcript abundance estimation. *Nat. Biotechnol.* **2016**, *34*, 1287–1291. [CrossRef] [PubMed]
145. Menyhart, O.; Weltz, B.; Győrffy, B. MultipleTesting.com: A tool for life science researchers for multiple hypothesis testing correction. *PLoS ONE* **2021**, *16*, e0245824. [CrossRef] [PubMed]
146. Kanduri, C.; Mamica, M.; Olstad, E.W.; Zucknick, M.; Li, J.J.; Sandve, G.K. Beware of counter-intuitive levels of false discoveries in datasets with strong intra-correlations. *Genome Biol.* **2025**, *26*, 249. [CrossRef] [PubMed]
147. Xue, C.; Chu, Q.; Shi, Q.; Zeng, Y.; Lu, J.; Li, L. Wnt signaling pathways in biology and disease: Mechanisms and therapeutic advances. *Signal Transduct. Target. Ther.* **2025**, *10*, 106. [CrossRef] [PubMed]
148. Maman, E.; Yung, Y.; Cohen, B.; Konopnicki, S.; Dal Canto, M.; Fadini, R.; Kanety, H.; Kedem, A.; Dor, J.; Hourvitz, A. Expression and regulation of sFRP family members in human granulosa cells. *Mol. Hum. Reprod.* **2011**, *17*, 399–404. [CrossRef] [PubMed]
149. Dombre, C.; Guyot, N.; Moreau, T.; Monget, P.; Da Silva, M.; Gautron, J.; Réhault-Godbert, S. Egg serpins: The chicken and/or the egg dilemma. *Semin. Cell Dev. Biol.* **2017**, *62*, 120–132. [CrossRef] [PubMed]
150. Silverman, G.A.; Whisstock, J.C.; Askew, D.J.; Pak, S.C.; Luke, C.J.; Cataltepe, S.; Irving, J.A.; Bird, P.I. Human clade B serpins (ov-serpins) belong to a cohort of evolutionarily dispersed intracellular proteinase inhibitor clades that protect cells from promiscuous proteolysis. *Cell. Mol. Life Sci.* **2004**, *61*, 301–325. [CrossRef] [PubMed]
151. Zhang, G.X.; Fan, Q.C.; Wang, J.Y.; Zhang, T.; Xue, Q.; Shi, H.Q. Genome-wide association study on reproductive traits in Jinghai Yellow Chicken. *Anim. Reprod. Sci.* **2015**, *163*, 30–34. [CrossRef] [PubMed]
152. Zhang, T.; Chen, L.; Han, K.; Zhang, X.; Zhang, G.; Dai, G.; Wang, J.; Xie, K. Transcriptome analysis of ovary in relatively greater and lesser egg producing Jinghai Yellow Chicken. *Anim. Reprod. Sci.* **2019**, *208*, 106114. [CrossRef] [PubMed]
153. Zhong, C.; Wang, Y.; Liu, C.; Jiang, Y.; Kang, L. A Novel single-nucleotide polymorphism in *WNT4* promoter affects its transcription and response to FSH in chicken follicles. *Genes* **2022**, *13*, 1774. [CrossRef] [PubMed]
154. Tai, Y.; Yang, X.; Han, D.; Xu, Z.; Cai, G.; Hao, J.; Zhang, B.; Deng, X. Transcriptomic diversification of granulosa cells during follicular development between White Leghorn and Silky Fowl hens. *Front. Genet.* **2022**, *13*, 965414. [CrossRef] [PubMed]
155. Sun, X.; Chen, X.; Zhao, J.; Ma, C.; Yan, C.; Liswaniso, S.; Xu, R.; Qin, N. Transcriptome comparative analysis of ovarian follicles reveals the key genes and signaling pathways implicated in hen egg production. *BMC Genom.* **2021**, *22*, 899. [CrossRef] [PubMed]
156. Li, Q.; Zuo, L.L.; Lin, Y.Q.; Xu, Y.O.; Zhu, J.J.; Liao, H.H.; Lin, S.; Xiong, X.R.; Wang, Y. Cloning and expression of *SFRP5* in Tibetan chicken and its relationship with IMF deposition. *Anim. Biotechnol.* **2016**, *27*, 231–237. [CrossRef] [PubMed]
157. de Almeida, L.G.; Thode, H.; Eslambolchi, Y.; Chopra, S.; Young, D.; Gill, S.; Devel, L.; Dufour, A. Matrix metalloproteinases: From molecular mechanisms to physiology, pathophysiology, and pharmacology. *Pharmacol. Rev.* **2022**, *74*, 714–770. [CrossRef] [PubMed]
158. Yuan, Z.; Chen, Y.; Chen, Q.; Guo, M.; Kang, L.; Zhu, G.; Jiang, Y. Characterization of chicken *MMP13* expression and genetic effect on egg production traits of its promoter polymorphisms. *G3* **2016**, *6*, 1305–1312. [CrossRef] [PubMed]
159. Zhu, G.; Jiang, Y. Polymorphism, genetic effect and association with egg production traits of chicken matrix metalloproteinases 9 promoter. *Asian-Australas. J. Anim. Sci.* **2014**, *27*, 1526–1531. [CrossRef] [PubMed]
160. Hogg, K.; Etherington, S.L.; Young, J.M.; McNeilly, A.S.; Duncan, W.C. Inhibitor of differentiation (Id) genes are expressed in the steroidogenic cells of the ovine ovary and are differentially regulated by members of the transforming growth factor-β family. *Endocrinology* **2010**, *151*, 1247–1256. [CrossRef] [PubMed]
161. Lorda-Díez, C.I.; Torre-Pérez, N.; García-Porrero, J.A.; Hurlé, J.M.; Montero, J.A. Expression of *Id2* in the developing limb is associated with zones of active BMP signaling and marks the regions of growth and differentiation of the developing digits. *Int. J. Dev. Biol.* **2009**, *53*, 1495–1502. [CrossRef] [PubMed]
162. Wang, L.H.; Baker, N.E. E proteins and ID proteins: Helix-loop-helix partners in development and disease. *Dev. Cell* **2015**, *35*, 269–280. [CrossRef] [PubMed]
163. Roschger, C.; Cabrele, C. The Id-protein family in developmental and cancer-associated pathways. *Cell Commun. Signal.* **2017**, *15*, 7. [CrossRef] [PubMed]
164. Zhu, G.; Fang, C.; Li, J.; Mo, C.; Wang, Y.; Li, J. Transcriptomic diversification of granulosa cells during follicular development in chicken. *Sci. Rep.* **2019**, *9*, 5462. [CrossRef] [PubMed]
165. Hosseinzadeh, S.; Hasanpur, K. Gene expression networks and functionally enriched pathways involved in the response of domestic chicken to acute heat stress. *Front. Genet.* **2023**, *14*, 1102136. [CrossRef] [PubMed]
166. Alsaeedi, A.H.; Al-Mahmood, H.H.R.; Alnaseri, Z.F.; Aziz, M.R.; Al-Shammary, D.; Ibaida, A.; Ahmed, K. Fractal feature selection model for enhancing high-dimensional biological problems. *BMC Bioinform.* **2024**, *25*, 12. [CrossRef] [PubMed]
167. van Rooij, M.M.; Nash, B.A.; Rajaraman, S.; Holden, J.G. A fractal approach to dynamic inference and distribution analysis. *Front. Physiol.* **2013**, *4*, 1. [CrossRef] [PubMed]

168. Zola, R.S.; Lenzi, E.K.; da Silva, L.R.; Lenzi, M.K. Entropy production in a fractal system with diffusive dynamics. *Entropy* **2023**, *25*, 1578. [CrossRef] [PubMed]
169. Chen, L.; Li, X.; Wu, Y.; Wang, J.; Pi, J. Differential analysis of ovarian tissue between high and low-yielded laying hens in the late laying stage and the effect of LECT2 gene on follicular granulosa cells proliferation. *Mol. Biol. Rep.* **2024**, *51*, 240. [CrossRef] [PubMed]
170. Karperien, A.L.; Jelinek, H.F. Box-counting fractal analysis: A primer for the clinician. *Adv. Neurobiol.* **2024**, *36*, 15–55. [CrossRef] [PubMed]
171. Volov, V.T. Fractal-cluster theory and its applications for the description of biological organisms. *Entropy* **2023**, *25*, 1433. [CrossRef] [PubMed]
172. Zhu, G.; Mao, Y.; Zhou, W.; Jiang, Y. Dynamic changes in the follicular transcriptome and promoter DNA methylation pattern of steroidogenic genes in chicken follicles throughout the ovulation cycle. *PLoS ONE* **2015**, *10*, e0146028. [CrossRef] [PubMed]
173. Barabasi, A.L.; Oltvai, Z.N. Network biology: Understanding the cell's functional organization. *Nat. Rev. Genet.* **2004**, *5*, 101–113. [CrossRef] [PubMed]
174. Naraine, R.; Abaffy, P.; Sidova, M.; Tomankova, S.; Pocherniaieva, K.; Smolik, O.; Kubista, M.; Psenicka, M.; Sindelka, R. NormQ: RNASeq normalization based on RT-qPCR derived size factors. *Comput. Struct. Biotechnol. J.* **2020**, *18*, 1173–1181. [CrossRef] [PubMed]
175. Wang, H.; Owens, J.D.; Shih, J.H.; Li, M.-C.; Bonner, R.F.; Mushinski, J.F. Histological staining methods preparatory to laser capture microdissection significantly affect the integrity of the cellular RNA. *BMC Genom.* **2006**, *7*, 97. [CrossRef] [PubMed]

Disclaimer/Publisher's Note: The statements, opinions and data contained in all publications are solely those of the individual author(s) and contributor(s) and not of MDPI and/or the editor(s). MDPI and/or the editor(s) disclaim responsibility for any injury to people or property resulting from any ideas, methods, instructions or products referred to in the content.